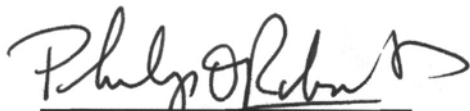


OCEAN DRILLING PROGRAM
LEG 127 PRELIMINARY REPORT
JAPAN SEA

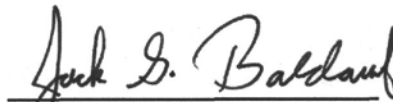
Dr. Kenneth Pisciotto
Co-Chief Scientist, Leg 127
7547 Terrace Drive
El Cerrito, California 94530

Dr. Kensaku Tamaki
Co-Chief Scientist, Leg 127
Ocean Research Institute
University of Tokyo
1-15-1 Minamidai, Nakano-ku
Tokyo 164, Japan

Dr. James F. Allan
Staff Scientist, Leg 127
Ocean Drilling Program
Texas A&M University
College Station, Texas 77840



Philip D. Rabinowitz
Director
ODP/TAMU



Jack G. Baldauf
Assistant Manager,
Science Operations
ODP/TAMU



Louis E. Garrison
Deputy Director
ODP/TAMU

September 1989

This informal report was prepared from the shipboard files by the scientists who participated in the cruise. The report was assembled under time constraints and is not considered to be a formal publication which incorporates final works or conclusions of the participating scientists. The material contained herein is privileged proprietary information and cannot be used for publication or quotation.

Preliminary Report No. 27

First Printing 1989

Distribution

Copies of this publication may be obtained from the Director, Ocean Drilling Program, Texas A&M University Research Park, 1000 Discovery Drive, College Station, Texas 77840. In some cases, orders for copies may require payment for postage and handling.

DISCLAIMER

This publication was prepared by the Ocean Drilling Program, Texas A&M University, as an account of work performed under the international Ocean Drilling Program, which is managed by Joint Oceanographic Institutions, Inc., under contract with the National Science Foundation. Funding for the program is provided by the following agencies:

Canada/Australia Consortium for the Ocean Drilling Program
Deutsche Forschungsgemeinschaft (Federal Republic of Germany)
Institut Français de Recherche pour l'Exploitation de la Mer (France)
Ocean Research Institute of the University of Tokyo (Japan)
National Science Foundation (United States)
Natural Environment Research Council (United Kingdom)
European Science Foundation Consortium for the Ocean Drilling Program
(Belgium, Denmark, Finland, Iceland, Italy, Greece, the Netherlands,
Norway, Spain, Sweden, Switzerland, and Turkey)

Any opinions, findings and conclusions or recommendations expressed in this publication are those of the author(s) and do not necessarily reflect the views of the National Science Foundation, the participating agencies, Joint Oceanographic Institutions, Inc., Texas A&M University, or Texas A&M Research Foundation.

SCIENTIFIC REPORT

The scientific party aboard *JOIDES Resolution* for Leg 127 of the Ocean Drilling Program consisted of:

- Kenneth Pisciotto, Co-Chief Scientist (7547 Terrace Drive, El Cerrito, California 94530)
Kensaku Tamaki, Co-Chief Scientist (Ocean Research Institute, University of Tokyo, 1-15-1 Minamidai, Nakano-ku, Tokyo 164, Japan)
James Allan, ODP Staff Scientist (Ocean Drilling Program, 1000 Discovery Drive, Texas A&M University, College Station, Texas 77840)
Joanne M. Alexandrovich (Lamont-Doherty Geological Observatory, Palisades, New York 10964)
David A. Barnes (Department of Geology, Western Michigan University, Kalamazoo, Michigan 49008)
Sam Boggs (Department of Geological Sciences, University of Oregon, Eugene, Oregon 97403)
Hans-Jürgen Brumsack (Geochemisches Institut, Goldschmidtstr. 1, D-3400 Göttingen, Federal Republic of Germany)
Charlotte A. Brunner (Center for Marine Science, University of Southern Mississippi, Stennis Space Center, Mississippi 39529)
Adrian Cramp (Department of Earth Sciences, University College, Swansea, United Kingdom; effective Sept. 1, 1989: Department of Geology, University College, Cardiff, P.O. Box 914, Cardiff CF1 34E, United Kingdom)
Laurent Jolivet (Department of Geology, Ecole Normale Supérieure, 24 rue Lhomond, 75005 Paris, France)
Orest E. Kawka (College of Oceanography, Oregon State University, Oceanography Administration Building 104, Corvallis, Oregon 97331-5503)
Itaru Koizumi (Institute of Geological Sciences, College of General Education, Osaka University, Toyonaka, Osaka 560, Japan)
Shin'ichi Kuramoto (Ocean Research Institute, University of Tokyo, 1-15-1 Minamidai, Nakano-ku, Tokyo 164, Japan)
Marcus Langseth (Lamont-Doherty Geological Observatory, Palisades, New York 10964)
James McEvoy (School of Ocean Sciences, University College of North Wales, Menai Bridge, Anglesey LL59 5EY, United Kingdom)
Jeffrey A. Meredith (Earth Resources Laboratory, Massachusetts Institute of Technology, 42 Carleton Street, Cambridge, Massachusetts 02142)
Karl A. Mertz Jr. (Department of Geology, Miami University, Oxford, Ohio 45056)
Richard W. Murray (Room 301, ESB, Department of Geology and Geophysics, University of California, Berkeley, California 94720)
David C. Nobes (Department of Earth Sciences and Department of Physics, University of Waterloo, Waterloo, Ontario, Canada N2L 3G1)
Atiur Rahman (Department of Geology and Geophysics, University of Utah, 717 W.C. Browning Building, Salt Lake City, Utah 84112-1183)
Ralph Schaar (Lamont-Doherty Geological Observatory, Palisades, New York 10964)

Kathryn P. Stewart (Department of Geology and Geophysics, University of Adelaide, G.P.O.
Box 498, Adelaide, South Australia 5001)

Ryuji Tada (Geological Institute, University of Tokyo, 7-3-1 Hongo, Tokyo 113, Japan)

Peter Thy (NASA, Johnson Space Center SN2, Houston, Texas 77058)

Luigi Vigliotti (Istituto Di Geologia Marina, Via Zamboni 65, I 40127 Bologna, Italy)

Lisa D. White (Earth Sciences Board, University of California at Santa Cruz, Santa Cruz,
California 95064)

Jobst J.M. Wipperfurth (Institut für Geophysik, Universität München, Theresienstr. 41/IV, 8000
München 2, Federal Republic of Germany)

Shigeru Yamashita (Earthquake Research Institute, University of Tokyo, Bunkyo-ku, Tokyo 113,
Japan)

ABSTRACT

Leg 127 of the Ocean Drilling Program was aimed at determining the rifting and bathymetric history of the eastern Japan Sea, as well as determining the previously unknown nature of its acoustic basement. Ten holes at four sites were drilled into the margins of the Japan and Yamato Basins, with three sites (Sites 794, 795, and 797) penetrating acoustic basement. Drilling at Sites 794 and 797 in the Yamato Basin showed that sediments in the basin are underlain by a sediment/basaltic-doleritic sill complex at least 350 m thick, whereas acoustic basement at Site 795 in the northern Japan Basin is composed of calc-alkaline basalt and basaltic andesite lava flows. Drilling results in the Yamato Basin confirm that the southeastern Japan Sea formed by rifting of a continental arc, with rifting underway by 19 Ma (early Miocene). Initial rifting was accompanied by intrusion and eruption of alkali and high-alumina basalts associated with deltaic or shallow-marine clastic deposits. Subsidence then followed rapidly, and the basin widened and deepened in the late middle Miocene with intrusion and extrusion of increasingly tholeiitic basalts for at least another 3.5 m.y. In contrast, basement at Site 795 is only ~14 Ma in age. Hemipelagic sedimentation followed rifting at all sites, depositing fine-grained claystones. During the late Miocene and Pliocene subsidence continued with extensive amounts of diatomaceous sediment deposited throughout the Japan Sea. Conditions changed in the latest Pliocene and in the Pleistocene, resulting in deposition of laminated light- and dark-colored silty clays punctuated by volcanic ash layers. Terrestrial and biogenic sedimentary input fluctuated widely during this time. Drilling at Site 796 on the Okushiri Ridge showed conclusively that compressive tectonics began to collapse the northeast margin of the Japan Sea beginning about 1.8 Ma, possibly representing initiation of a new subduction zone. Associated with this upthrust feature is the highest heat flow ever obtained in the Japan Sea (156 mW/m²). Thus, drilling on Leg 127 has documented both the initiation of formation of the Japan Sea and the initiation of its possible destruction.

INTRODUCTION

The Japan Sea is one of the most intensively studied marginal seas in the western Pacific region (Tamaki, 1988). It consists of several deep basins (water depths in excess of 3000 m) which appear to be floored by oceanic-type crust and separated by ridges underpinned by continental material (Fig. 1). This general picture has been developed from an extensive marine geophysical data base but suffers from a lack of hard geological data on the acoustic basement aside from that gained from dredging operations. Most tectonic models consider the sea to represent a backarc basin initiated by multiple rifting probably during the late Oligocene-early/middle Miocene.

The overall goals of the drilling program for ODP Leg 127 included documentation of the tectonic, depositional, and paleoceanographic development of the Japan Sea. Specific goals included (1) determination of the nature and age of basal basement, (2) determination of the tectonic manner in which the Japan Sea rifted open, (3) determination of the age of the onset of convergence in the northeast Japan Sea, and (4) acquisition of downhole measurements that would help to constrain the Japan Sea stress environment.

GEOLOGIC FRAMEWORK

Tectonics and Structure

The Japan Sea lies between the subduction zones of the western Pacific and the Himalayan convergence. At least four major plates and several microplates converge in this area (Fig. 2). The Japan Sea lies principally on the Eurasian plate (or Amurian microplate) and is separated from the North American plate (or Okhotsk microplate) on the east-northeast by a young plate boundary characterized by active thrust faulting and large ($M > 7$), compressional earthquakes (Fukao and Furumoto, 1975; Kimura and Tamaki, 1986).

Patterns of faulting and the shallow structure of the Japan Sea are known from seismic reflection data (Tamaki, 1988). At least three structural provinces exist: (1) basinal areas, such as the Japan and Yamato basins, containing mostly flat-lying sediments over a moderately irregular acoustic basement surface; (2) block-faulted ridges underpinned by continental and rifted continental rocks, as typified by the Yamato Rise, Korea Plateau, Ullung Rise, and Oki Bank; and (3) a compressional northeastern margin displaying complex folding and uplifted tectonic ridges bounded by young thrust faults. Based on DSDP Leg 31 drilling (Karig, Ingle, et al., 1975), upper Miocene hemipelagic sediments drape the block-faulted acoustic basement of the Yamato Rise, indicating that the initial extension is probably no younger than about 10 Ma. In contrast, the thrust faults and folds occurring along the eastern margin of the Japan Sea are very young. Seismic stratigraphic data indicate that much of the folding probably occurred in the late Pliocene-Pleistocene, and modern seismicity demonstrates that the thrust faults are currently active (Seno and Eguchi, 1983; Kimura and Tamaki, 1986; Yamazaki et al., 1985).

Seismic refraction data (Ludwig et al., 1975) show that velocities and thicknesses fairly typical of oceanic crust prevail in the center of the Japan Basin, whereas both layers 2 and 3 of the Yamato Basin are thicker than typical oceanic crust. Quaternary volcanism is largely confined to the Japanese Islands and the eastern Japan Sea margin and is a consequence of continued westward subduction of the Pacific and Philippine plates (Tamaki, 1988). Westward of this broad arc lie several chains of andesitic seamounts, mostly of Miocene age. Heat flow in the Japan Sea ranges from 53 to 138 mW/m², with the bulk of values lying between 74 to 115 mW/m² (Yoshii and Yamano, 1983; Tamaki, 1986).

Sedimentary and Paleoceanographic Summary

Neogene and Quaternary sediments present in basinal areas of the Japan Sea locally reach thicknesses of 1500-2000 m (Ludwig et al., 1975; Gnibidenko, 1979; Tamaki, 1988). Seismic data, and limited stratigraphic data from DSDP Leg 31 sites (Karig, Ingle, et al., 1975), illustrate that a similar stratigraphic sequence characterizes most basinal areas despite significant differences in sediment thickness (Ishiwada et al., 1984; Kobayashi, 1985). This typical basinal sequence consists of an upper well-stratified and highly reflective unit composed of Pliocene to Holocene siliciclastic sands, silts, and/or clays overlying a seismically transparent unit of lower Pliocene to Miocene hemipelagic diatomaceous silts and clays. This sequence represents a major change from widespread deposition of Miocene-lowermost Pliocene hemipelagic sediments to a basin-filling facies involving rapidly deposited Pliocene to Holocene siliciclastic turbidites (Ingle, 1975).

SITE-SPECIFIC DRILLING OBJECTIVES

Sites 794 and 797 (Yamato Basin)

Site 794 (proposed site J1B-1; 40°11.40'N, 138°13.86'E; 2811 m water depth), located in the northern Yamato Basin, was designed as a reentry hole that would penetrate 620 m of sediment and continue at least 100 m into acoustic basement (Fig. 1). Reentry was planned to ensure maximum basement penetration and to provide an open hole for later downhole experiments during Leg 128. The principal objective of this site was to determine the nature and age of the basement rocks. Recent seismic refraction data indicate an anomalously thick oceanic crust throughout much of the Yamato Basin, and a detailed magnetic survey suggests a complex pseudofault pattern indicative of frequent ridge propagation during basinal spreading. Basement sampling at Site 794 will permit a determination of the age and nature of the anomalous crust and improve our understanding of the style and mechanisms of backarc extension in this area.

In addition to the basement sampling at this site, continuous coring of the sedimentary section will complement the findings at DSDP Site 299, where the lower part of the sedimentary section was not penetrated. These data will provide facies and paleoceanographic information at a basinal site in the Japan Sea and, through regional seismic correlations, will be useful in understanding the style and evolution of sedimentation in this backarc setting.

Site 797 (proposed site J1E-1; 38°36.96'N, 134°32.16'E; 2862 m water depth) is located in the west-central Yamato basin south and east of the Yamato Rise (Fig. 1). The objectives at this site were the same as at Site 794, namely (1) determination of the age and nature of basement, (2) style of multiple rifting, and (3) characterization of the sedimentary history. Drilling was proposed to a total depth of 720 m, which included 50 m of basement penetration.

Site 795 (Japan Basin)

Site 795 (proposed site J1D-2; 43°59.22'N, 138°57.90'E; 3300 m water depth) is located at the northern end of the Japan Basin (Fig. 1). The original plan was to penetrate 630 m of sediment and 50 m of acoustic basement. As at the previous sites, the objectives were to determine the nature and age of the basement for tectonic interpretations and to characterize the sedimentation history of the Japan Basin. This site represents the first DSDP/ODP site in this part of the Japan Sea and as such will complement the results from the southern sites.

Site 796 (Okushiri Ridge)

Site 796 (proposed site J3B-1; 42°50.94'N, 139°24.84'E; 2571 m water depth) is located on the Okushiri Ridge, a complex, thrust-faulted structure along the northeastern flank of the Japan Basin. It has been proposed that this ridge represents an obducted block formed by compression associated with backarc spreading (Tamaki, 1988). The principal goals of the drilling at this site were to (1) constrain the timing of uplift and compressional tectonics in this area, (2) provide data on the nature and age of the uplifted basement, and (3) characterize the sedimentary history for paleoceanographic reconstructions.

DRILLING RESULTS

The unifying objective of drilling in the Japan Sea was to assess the style and dynamics of rifting and marginal sea formation in a continental arc setting. The specific objectives at Sites 794, 795, and 797 were to (1) determine the nature and age of the basement, (2) measure the direction of the present stress field, and (3) characterize the sedimentation, subsidence, and oceanographic evolution of the Yamato and Japan Basins. Site 796 shared these objectives, but was also designed to constrain the age of initiation of basinal compression along the northeast margin of the Japan Sea. Leg 127 extended over a period of 63.0 days, of which 4.4 days were spent in port, 9.3 days were spent surveying and under way, and 49.3 days were spent on site, of which 8.6 days were devoted to downhole science and logging. A total of 318 cores were taken, representing 1655.2 m of recovered core. The total downhole distance cored was 2917.2 m, so recovery was a respectable 56.7%. Figure 3 shows a summary of the lithology cored at the four sites.

Site 794

Principal Results

1. A dolerite sill complex was encountered in the deepest penetration. The age of the claystone above the uppermost sill gives a minimum age of basin initiation at this site of 14.5 - 16.5 Ma. The exact age and nature of basement, however, is still uncertain because (a) the tuff and claystone beneath the 110-m-thick interval of dolerite sills could not be dated, and (b) the acoustically opaque seismic interval, which underlies the highly reflective dolerite sill complex and may represent true basement, has not yet been penetrated.

2. The in-situ stress field is not yet known because the logging and packer tools used to make the measurements could not be run past the stuck pipe in Hole 794C.

3. The sedimentary and paleontologic sequences indicate that this area of the northern Yamato Basin evolved in three stages: (a) a middle Miocene period characterized by bioturbated, hemipelagic claystones, gravity-flow tuffs, and minor glauconite and phosphorite, deposited at upper bathyal depths (~500 m) in suboxic marine waters on a slope or borderland ridge; followed by (b) subsidence to lower bathyal depths (>~1500 m) during the late middle Miocene with deposition of hemipelagic diatomaceous sediments and increasing amounts of volcanic ash through the early Pliocene in cool, well-oxygenated waters; and finally (c) a late Pliocene to Holocene period in which diatomaceous sedimentation shut down, volcanic ash production increased, and oscillating climate and tectonism produced interbedded, massive, and laminated hemipelagic sediments. Except for parts of the Quaternary, preservation of primary biogenic carbonate is poor, suggesting a consistently shallow CCD (<1500 m) or dissolution during early diagenesis. Dissolution of siliceous microfossils is also widespread. Silica diagenetic transitions of opal-A/opal-CT and opal-CT/quartz were well identified by lithology, geochemistry of sediments and interstitial water, physical-property measurements, and logging data. The opal-A/opal-CT transition shows up clearly as a widespread bottom-simulating reflector that can be traced extensively.

Lithology

The sedimentary section cored in Holes 794A and 794B consists mostly of fine-grained hemipelagic sediments of Quaternary to early middle/late early Miocene age. Tuffs and tuffaceous sediments were recovered from Hole 794C between dolerite sills. The division of sedimentary units is as follows:

Unit I: 0-92.3 mbsf; 0-3.0 Ma. Clay and Silty Clay. The upper 63.8 m consists of alternating light bioturbated zones and dark laminated zones with common thin ash layers. The lower 28.5 m is similar to the upper interval but with fewer dark zones. Diatoms increase downsection.

Unit II: 92.3-293.5 mbsf; 3.0-8.1 Ma. Diatomaceous Ooze and Clay. The upper 201.2 m consists of bioturbated ooze and clayey ooze with sparse ash layers. Diatomaceous clay makes up the lower 76.6 m. Diatoms decrease and opal-CT cement increases in this interval.

Unit III: 293.5-491.7 mbsf; 8.1-~14.6 Ma. Clay and Claystone. The upper 57.8 m is bioturbated clay and claystone with minor ash, pyrite, and micritic carbonate. The lower 140.3 m is bioturbated claystone with rare laminated intervals. Porcellanites occur at several levels and dolomitic, sideritic, siliceous cements and phosphatic lenses are common.

Unit IV: 491.7-520.6 mbsf; ~14.6-15.8 Ma. Tuff and Claystone. This unit consists of interbedded tuff, lapilli tuff, and claystone. The tuffs are variously thin- to thick-bedded, normal to inversely graded with sharp basal contacts. Some beds contain planar, convolute, and cross laminations. Others contain burrowed intervals and are massive and poorly sorted with claystone fragments. Interbedded claystones are moderately bioturbated.

Unit V: 520.6-543 mbsf; ~15.8-16.5 Ma. Claystone. This unit consists of interbedded claystones of variable compositions with minor interbedded tuff. From top to bottom, silty claystone, phosphatic claystone, and black claystone are the dominant lithologies. Minor thin intervals and lenses of glauconitic claystone, pelletal phosphorite, and pyrite are also present in these moderately bioturbated claystones. Sparse, thin tuff layers display cross laminations and flame structures. (Igneous rocks fill the interval 543-644.1 mbsf.)

Unit VI: 644.1-645.6 mbsf; (age unknown). Tuff and Tuffaceous Claystone. This unit is separated from Unit V by 100 m of dolerite. It consists of bioturbated claystone and massive to laminated, fine-grained tuff. The tuff also shows convolute laminations, small slump folds, normal size grading, and bioturbated tops.

Age and Sedimentation Rate

The ages of sediments are well constrained by diatom zones in Unit I and Unit II (0-293.5 mbsf). Below this level, the diatoms decrease in abundance; the coincident increase in opal-CT indicates dissolution of diatoms owing to burial diagenesis. Foraminifers, nannofossils, and radiolarians occur sporadically throughout these cores. Where present, they confirm diatom dates, but because of poor preservation and/or sparse populations, they do not add accuracy or precision. In contrast, a good paleomagnetic reversal record is present from the Brunhes to almost the bottom of the Gilbert chron (~5 Ma at 150 mbsf), giving precise time correlation from the Pleistocene to the Pliocene. Below Unit III (491.7 mbsf), only sparse, poorly preserved calcareous nannofossils and planktonic foraminifers provide age control. The oldest paleontological age assigned is 15.8-16.5 Ma for the claystone overlying the dolerite (530.3 - 543 mbsf). Using all of the age data, the

sedimentation rates are (1) 30 m/m.y. for the Pleistocene - early Pliocene (0-4.8 Ma), (2) 45 m/m.y. for the early Pliocene to late Miocene (4.8-9.4 Ma), and (3) 30 m/m.y. for the early late Miocene - early middle to late early Miocene (9.4-16 Ma). These rates were computed using present-day compacted sediment thicknesses.

Geochemistry

Sediments from Holes 794A and 794B are characterized by low organic carbon contents (TOC: range 0.1-3.0%; average 0.7%) and by increases in diagenetic silica, dolomite, and phosphate with depth, particularly below 300 mbsf. Diatoms (opal-A) and volcanic glass decrease markedly below this level. Biogenic carbonate is sparse throughout much of the sediment column. Interstitial-water profiles also show pronounced gradient changes below 300 mbsf. In particular, Ca increases and Mg, K, and Li decrease sharply coincident with diagenesis of the sediments. Sulfate is present throughout, indicating that the entire section is within the zone of sulfate reduction. Virtually no hydrocarbon gases were detected. Methane levels from headspace analysis were only a few parts per million and are indistinguishable from background levels measured in the shipboard laboratory. No gas was observed in core liners, and this was confirmed by the vacutainer gas samples. No safety problems related to gas were encountered at this site.

Igneous Rocks

Dolerite was the principal igneous rock type recovered in Holes 794B and 794C. Penetration below the first contact between the dolerite and sediments (543 mbsf) was 6 m in Hole 794B and 109.4 m in Hole 794C. A total of 34.5 m of rock was recovered below this contact (including sedimentary Unit VI: 1.5 m thick, 644.1-645.6 mbsf). The igneous rocks were divided into six units based on chemistry and texture as shown below. The upper two units have rather high acoustic velocities (4.6-5.2 km/s) compared to the lower units (3.5 - 4.3 km/s). Each unit is thought to represent a separate intrusive sill. Most of the igneous rocks are highly altered, and the ages are unknown.

Unit 1: 543-549 mbsf. Moderately Plagioclase Phyric Dolerite. A horizontal contact is observed at the top of this unit, with a thin zone of baked clay sediment above and a chilled margin of moderately plagioclase phyric basalt below.

Unit 2: 560-601 mbsf. Moderately to Highly Plagioclase Phyric Dolerite. This unit is primarily massive and dense, with some highly fractured intervals.

Unit 3: 601-623 mbsf. Aphyric Dolerite. This unit is moderately vesicular, massive, and highly fractured.

Unit 4: 623-634 mbsf. Aphyric Dolerite. This unit is composed of massive, vesicular, medium- to fine-grained aphyric dolerite. The upper half of the unit is highly fractured, whereas the lower half has few fractures.

Unit 5: 634-644 mbsf. Aphyric Dolerite. This unit is highly vesicular. The lower boundary of the unit is sharply defined by a baked contact with tuffaceous sediments. (One meter of sediment intervened between Units 5 and 6.)

Unit 6: 645-646 mbsf. Aphyric Basalt. The top of this unit is a chilled, intrusive margin against baked and welded tuff in sedimentary Unit VI.

Seismic Stratigraphy

Six distinct seismic intervals occur at the site. From top to bottom they are (1) an upper well-stratified interval, (2) a transparent or faintly-stratified interval, (3) a middle well-stratified interval, (4) a lower moderately well-stratified interval, (5) a lowermost highly reflective interval, and (6) an unstratified, acoustically opaque zone. Interval 1 correlates to Unit I and the upper part of Unit II. Interval 2 correlates to the lower part of Unit II. Interval 3 corresponds to the upper part of Unit III; its top is coincident with the opal-A/opal-CT transition. Interval 4 corresponds to the lower part of Unit III and all of Units IV and V. Interval 5 includes igneous Units 1 through 6 and interbedded sedimentary Unit VI. Seismic interval 6 corresponds to acoustic basement, which was not penetrated in Holes 794A, 794B or 794C.

Heat Flow

Successful temperature measurements were made using the Uyeda probe at 10 points down to 351 mbsf in Hole 794A. The measured temperature gradient was 125°C/km. The calculated heat-flow value using this gradient and measured thermal conductivities is 103 mW/m². This value matches the average heat-flow value of the Yamato Basin (97 ±12 mW/m²).

Logging

Three successful logging runs were completed in Hole 794B (combination sonic/lithodensity/temperature/DIT, geochem, and FMS). The combination of the tool lengths and shallow basement penetration (5 m) did not permit logging of the basement/sediment contact. The maximum reach of the bottom of the tool was 1 m above the contact. Of the data processed and examined to date, the resistivity, velocity, and bulk-density profiles characterize the sedimentary section. The boundary between Units II and III at 293 mbsf is clear on all three profiles. This corresponds to the opal-A/opal-CT transition. Another break occurs at about 400 mbsf, within Unit III at the opal-CT/quartz transition. Unit IV, the interval of tuff and claystone, shows up clearly between 490 and 520 mbsf as a zone of low density, velocity, and resistivity. Each of these parameters increases again below this in the dolerite interval.

Site 795

Principal Results

1. Basalts, basaltic andesites and basaltic breccias constitute acoustic basement at this locality. Textures, mineralogy, and chemistry indicate that these rocks contain calc-alkaline and volcanic arc affinities, quite different from rocks associated with seafloor spreading. They could be associated with either arc volcanism or with initial arc rifting. The sediment which immediately overlies these rocks gives a minimum age of basin initiation of 15.5 Ma.

2. The *in-situ* stress field could not be determined because of a blockage in the hole at 230 mbsf during downhole logging and packer/hydrofracture experiments.

3. The sedimentary and paleontologic sequences indicate a three-stage evolution of this part of the northern Japan Basin, which is broadly similar to that at Site 794: (a) a middle Miocene period beginning with explosive volcanism resulting in ash falls and submarine, gravity-flow tuffs, coincident with and followed by marine claystone deposition on a well-oxygenated to mildly disoxic

slope or basin which subsided from upper and mid-bathyal (~500-1000 m) to lower bathyal depths (~1500 m); then (b) a gradual increase in hemipelagic diatomaceous sedimentation, beginning in the late Miocene and culminating in the early Pliocene, in cool well-oxygenated waters; and finally (c) a late Pliocene to Holocene stage in which diatomaceous sedimentation pulsed, volcanic ash production increased, the climate cycled from arctic to subarctic conditions, and local tectonism produced complex interbedding of hemipelagic and terrigenous sediments that were deposited at nearly twice the rates found at Site 794. Except for episodes during the middle Miocene, early late Miocene, and late Pliocene through Quaternary, preservation of primary biogenic carbonate within the sediments is poor, indicating a consistently shallow CCD (<1500 m) or dissolution during early diagenesis. Dissolution of siliceous microfossils is also pronounced. The opal-A/opal-CT and opal-CT/quartz diagenetic transitions are well defined by lithology, geochemistry of sediments and interstitial water, and physical-properties data. The opal-A/opal-CT boundary corresponds to a widespread bottom-simulating reflector which locally cuts across stratal reflectors.

Lithology

The sedimentary section cored in Holes 795A and 795B consists mostly of fine-grained, diatomaceous hemipelagic and terrigenous sediments of middle Miocene to Quaternary age. The division of units is as follows:

Unit I: (0-123.0 mbsf; 0-2.1 Ma). Silty Clay and Clay. The upper 85 m is color-banded, light and dark silty clay, clay, diatomaceous clay, and minor ash. Subtle size grading occurs in the silty clays and ashes. Bioturbation is minimal. The lower 38 m is similar but with increasing diatom content and increased bioturbation.

Unit II: (123.0-239.0 mbsf; 2.1-4.0 Ma). Diatom Ooze, Diatom Silty Clay, and Diatom Mixed Sediment. This unit is distinguished from Unit I by a significant increase in diatom content. Minor ash layers are present, and the unit is moderately to extensively bioturbated.

Unit III: (239.0-325.0 mbsf; 4.0-5.4 Ma). Silty Diatom Claystone and Diatom-Clay-Silt Mixed Sediment. This unit is similar to Unit II but contains a lower diatom content and increased amounts of silt and clay. The lower 50 m of this unit contains slightly less clay than the upper part. Minor calcareous and dolomitic nodules are present. Bioturbation is common.

Unit IV: (325.0-665.0 mbsf; 5.4-~14.5 Ma). Siliceous Claystone and Silty Siliceous Claystone. The upper 146 m of this unit is opal-CT siliceous silty claystone with minor porcellanite, dolomite, and some chert. The lower 194 m consists of burrowed claystone with minor tuff and micrite layers, and pyritic and calcareous nodules. Opal-CT changes to quartz at ~471 mbsf, and the claystone becomes less siliceous below 560 mbsf. The cyclicity in the style of bioturbation increases with depth, as does the abundance of small faults and calcite- and clay-filled fractures. The tuff layers are normally graded with internal laminations and burrowed tops.

Unit V: (665.0-683.5 mbsf; ~14.5-~15.5 Ma). Claystone and Tuff. This unit overlies the basalt and basaltic breccia and consists of interbedded claystone and altered, fine- to coarse-grained tuff. These strata are commonly graded, laminated, and burrowed in the style of the overlying sediments. Small faults and clay-filled fractures are common in the claystone. Calcite-filled fractures occur in the tuff.

Age and Sedimentation Rates

The sediment ages are well constrained by diatom zones and paleomagnetism in Unit I, and by diatom zones in Units II and III (0-325 mbsf). Below this level, all diatoms, except those protected in calcareous concretions, have been dissolved. Units IV and V were dated primarily by using these sporadic protected samples, with sparse correlation by foraminifers, radiolarians, and calcareous nannofossils. The oldest paleontological age, 13.3 Ma, occurs at 635.5 mbsf. Summarizing all of the age data, uncompacted sedimentation rates are (1) 60 m/m.y. for the Pleistocene through latest Miocene (0-6.4 Ma), (2) 39 m/m.y. for most of the late Miocene (6.4-10.7 Ma), and (3) 29 m/m.y. for the middle Miocene (10.7-15.5 Ma).

Geochemistry

Sediments from Holes 795A and 795B are characterized by variable organic-carbon contents, particularly in the color-banded Pliocene-Pleistocene sediments (total organic carbon, or TOC, was 0.25-4.0%). The organic-matter type was principally terrestrial, although the Pliocene-Pleistocene portion of the section contained mixed terrestrial and marine algal sources. Methane occurred in low amounts from the seafloor to 80 mbsf. Below this level, methane increased sharply and ethane appeared, but quantities were still relatively low. Amounts of both gases increased slightly but steadily with depth to the basement. Sporadic traces of propane occurred below about 325 mbsf. No safety problems related to gas were encountered. The chemistry profiles of interstitial-water samples matched the observed sediment and organic-matter diagenesis. The base of the sulfate-reduction zone occurs at 80 mbsf, where methane increases. Dissolved silica increases to a maximum at the opal-A/opal-CT boundary (325 mbsf), then decreases sharply below, indicating silica precipitation. Dissolved Mg decreases linearly to basement. In contrast, dissolved Ca changes only slightly until the opal-A/opal-CT transition at 325 mbsf, where it increases sharply in concentration to the base of the sediment column.

Igneous Rocks

Basalt, basaltic andesites, and basaltic breccias comprise acoustic basement at this site. All rocks are moderately to highly altered and vesicular (5-30%). These are divided into three units on the basis of texture and mineralogy.

Unit 1: Brecciated sparsely plagioclase pyroxene phyric basaltic andesite; 683.5-703.3 mbsf.

Unit 2: Silicified brecciated moderately plagioclase phyric basalt; 703.3-704 mbsf.

Unit 3: Sparsely pyroxene plagioclase phyric basalt, 704-762.2 mbsf (total depth). This unit is further divided into two subunits: Unit 3A, predominantly massive basalt, 704-733.7 mbsf; and Unit 3B, predominantly brecciated basalt and basaltic andesite, 733.7-762.2 mbsf.

The igneous rocks are characterized by low amounts of large-ion lithophile elements (LILE; including K, Rb, Sr, and Ba), high-field strength elements (HFSE; including Nb, Zr, and Ti), and light rare-earth elements (LREE; Ce). They are all evolved, containing low amounts of Cr, Ni, and MgO. All Site 795 lavas, most notably the most evolved ones, contain high amounts of Al₂O₃. Their mineralogy and chemistry indicate that they have calc-alkaline and volcanic-arc affinities, yet their composition reflects little or no evidence of involvement of continental crust in their genesis. The Site 795 igneous rocks were erupted subaqueously. Constraints imposed by the immediately

overlying sediments indicate that they were erupted below wavebase (100-200 mbsl), yet the high vesicularity implies shallow water depth (probably above 1000 mbsl). They represent lavas erupted within a volcanic arc or backarc setting, and could be associated with the initial rifting of either an oceanic or continental volcanic arc.

Seismic Stratigraphy

Five distinct seismic intervals occur at this site. From top to bottom these are (1) an upper weakly stratified interval, (2) a transparent interval with partly hummocky reflectors, (3) a strongly stratified interval, (4) a lower moderately well-stratified interval, and (5) an unstratified, acoustically opaque zone. Interval 1 correlates with Unit I. Interval 2 correlates with the Units II and III. Interval 3 correlates with the upper part of Unit IV; its top is coincident with the opal-A/opal-CT diagenetic boundary. Interval 4 corresponds with the lower part of Unit IV and all of Unit V. Interval 5 corresponds to acoustic basement, which was penetrated in Hole 795B.

Heat Flow

Successful temperature measurements were made using the Uyeda probe at 5 points down to 162.4 mbsf in Hole 795A. The measured temperature gradient is 133°C/km. The calculated heat-flow value using this gradient and measured thermal conductivities is 113 mW/m². This value is slightly higher than the average value for this part of the Japan Basin (99 mW/m²).

Site 796

Principal Results

Site 796 is located on the eastward-dipping slope of the Okushiri Ridge in the eastern margin of the Japan Sea. This slope is estimated to have been formed by a westward-dipping thrust fault.

The specific objectives at this were to (1) determine the age and history of uplift of the ridge, (2) measure the direction of the present stress field, (3) determine the age and nature of basement; and (4) characterize the sedimentation and oceanographic evolution of the area.

Unfortunately penetration into basement was not attained (TD 465 mbsf, 100 m above basement) because of unstable hole conditions caused by shallow coarse sand beds and fractured rocks in the lower levels. As a result, objectives (2) and (3) were not achieved. The principal results at Site 796 are as follows:

1. The age of initiation of the uplift of Okushiri Ridge was determined by the shallowest appearing sand bed. The age of this shallowest sand is estimated by diatom stratigraphy to be 1.8 Ma. This observation suggests that the Okushiri Ridge (WD 2300 m) rose 1300 m above the Japan Basin floor (WD 3600 m) in 1.8 Ma at a rate of 0.7 mm/yr. As the uplift of Okushiri Ridge was caused by thrust activity along the eastern margin of the Japan Sea (a possible new Eurasian-North American plate boundary), these results provide the first exact age data on the initiation of the convergence along this margin and are critical to address the tectonics of this new plate boundary.

2. The lithology at Site 796 below the uppermost Pliocene is quite different from the previous two sites and is characterized by abundant input of coarse-grained clastic and pyroclastic detritus as sediment gravity-flow deposits, suggesting a marginal facies of a basin. Paleooceanographic conditions that are suggested by the sedimentary sequences and paleontological data, however, are approximately similar to those inferred at Sites 794 and 795. The calcium carbonate abundance in

the sediments and the microfossil preservation show that the site was above the CCD during the middle(?) Miocene and below it through the late Miocene to the Quaternary. The ubiquitous bioturbation observed throughout the sedimentary column shows that the sediments at Site 796 accumulated under oxic conditions. Interstitial-water geochemistry shows elemental depth variation, but these variations are well explained when correlated with lithology, especially ash beds and sand beds. No vertical fluid transport was suggested by the interstitial water geochemical data, whereas physical property data may suggest occurrence of some vertical fluid flux.

3. The highest heat flow ever obtained in the Japan Sea, 156 mW/m², was measured at Hole 796B. The associated high temperature gradient (178°C/km) is quite consistent with the shallow obscured opal-A/opal-CT transition zone (215 mbsf, 40°C). Frictional heating along the thrust faults is one potential source of excess heat, but frictional heat alone cannot account for this high heat flow. A mechanism to concentrate the heat flow, such as fluid flow along faults, is required to match the magnitude of the anomaly.

Lithology

The sedimentary section cored in Holes 796A and 796B differs from those at Sites 794 and 795 by exhibiting a significant input of terrigenous components during the late Miocene to Quaternary. Sand is first observed in Core 127-796A-9X (63 mbsf) and in Core 127-796B-7R (70 mbsf). In both holes, the shallowest sand appears in the uppermost part of the uppermost Pliocene strata (1.8-2.5 Ma). In Hole 796B, the age of the shallowest sand is constrained by diatoms to be 1.8 Ma. The opal-A/opal-CT transition was observed at 225 mbsf by XRD analyses.

The division of units is as follows:

Unit IA: (0-51.7 mbsf; 0-1.8 Ma). Clay and Silty Clay without sand. The unit is moderately to highly bioturbated, and associated with soft-sediment deformation by slumping and microfaults.

Unit IB: (51.7-146.2 mbsf; 1.8-4.1 Ma). Clay and Silty Clay with numerous sand beds. The number of soft-sediment deformation features decreases as compared to Subunit IA. Sand beds occur throughout the subunit as scattered thin beds (typically 1-10 cm thick, thickest 65 cm) that have sharp basal contacts. The sands are dominated by volcanic lithic fragments and pumice of fine to medium grain size.

Unit II: (146.2-223.5 mbsf; 4.1-5.9 Ma). Clayey Diatom Ooze and Diatom Claystone. The detrital input increases toward the base of unit with sandstone and pebbly claystone. Sandstone beds occur as thin (2-10 cm) graded units with sharp basal contacts and are dominantly composed of volcanic lithic fragments and glass or pumice.

Unit III: (223.5-301.0 mbsf; late Miocene). Siliceous Claystone, Claystone, and Sandstone.

Claystone units are moderately to highly bioturbated. Sandstone and siltstone interbeds are abundant in the middle part. Sandstones beds are graded, medium- to coarse-grained, with volcanic lithic detritus and glass shards. They range from a few centimeters to 60 cm in thickness. Scattered glauconite is also observed.

Unit IV: (301.0-416.5 mbsf; late Miocene?). Siliceous Claystone, Pebbly Claystone, Tuffaceous Sandstone, and Tuff. This unit is characterized by siliceous claystone interbedded with coarse-grained pyroclastic deposits consisting of sandstone and pebbly claystone with abundant

volcanic detritus and discrete tuff beds. The opal-CT/quartz diagenetic boundary is observed from 301 to 330 mbsf. The claystone is well bioturbated. Pebbly claystone commonly occurs through this unit and is matrix-supported, coarse sand- to pebble-size volcanic detritus that includes pumice, tuff, and other volcanic lithic fragments. Laminated tuffaceous sandstone is present as thin beds throughout the unit, and laminated, graded tuff beds (some exceeding 2 m in thickness) also occur.

Unit V: (416.5-464.9 mbsf; late-middle(?) Miocene). Siliceous Claystone and Silty Claystone.

This unit is distinguished from overlying strata by the paucity of coarse clastic/pyroclastic deposits and by an increase in dolomite and Mg-calcite. Siliceous claystones are generally bioturbated.

Age and Sediment-Accumulation Rates

Sediment ages are well constrained by diatom zones in Unit I, Unit II, and the uppermost part of Unit III (0-253 mbsf). Below this level, all diatoms have been dissolved. The paleomagnetic data as well as the other paleontological data were sparse and not usable to identify datums or determine ages. The oldest age determined was 6.4 Ma at 253 mbsf by the first-appearance datum (FAD) of the diatom *Neodenticulata kamtschatica*. The ages of Units IV and V were estimated solely by simple extrapolation of the sediment-accumulation curve. The estimated age of the bottom of the hole (465 mbsf) is 9.7 Ma based on this extrapolation. Uncompacted sedimentation rates are (1) 46 m/m.y. for the late Pleistocene (0-0.9 Ma), (2) 11 m/m.y. for the early Pleistocene (0.9-1.8 Ma), (3) 39 m/m.y. for most of the Pliocene (1.8-5.3 Ma), and (4) 62 m/m.y. (5.3-6.4 Ma) for the late Miocene (5.3-6.4 Ma).

Geochemistry

High methane concentrations were observed from 10 to 140 mbsf, ranging from 7300 to 830,000 ppm in the vacutainer samples. C1/C2 ratios in this interval were constantly above 1000, suggesting a biogenic source for this gas. Gas hydrate was observed in Core 127-796A-12X (~90 mbsf) and was sampled. Results of analysis of the clathrate show that the pore-water chemistry (salinity, NaCl, sulfate) at Site 796 was influenced by the presence of methane clathrates and that clathrates are probably present throughout the upper 120 m at this site. Below 200 mbsf, the methane concentration decreases to <100 ppm, and below 340 mbsf methane increases again to 1500-8200 ppm with only small amounts of ethane (1-16 ppm), suggesting a minor influx of thermogenic methane.

The Quaternary sediments above 70 mbsf vary in total organic carbon content (TOC), with TOC ranging between 0.34 and 4.0%, suggesting a rather prominent variation in paleoenvironment. The low TOC contents (<1.0%) below 70 mbsf indicate sediment deposition under highly oxygenated bottom-water conditions. The base of the sulfate reduction zone occurs at 14 mbsf, much shallower than at Site 795 (80 mbsf). Sulfate increases markedly again below 62 mbsf and attains a value of 20 mmol/L at 206 mbsf. Abundant ash layers in the upper 150 m controlled the behavior of the alkaline earth elements at this site, controlling in particular the extreme depletion of Mg. Careful examination of the pore-water chemistry does not show any positive evidence of fluid transport along possibly active faults.

Seismic Stratigraphy

The acoustic character of the sediments at Site 796 is totally opaque except for a thin interval in the lowermost portion of the section. Stratification is very poor. No clear bottom-simulating reflector associated with gas hydrate is observed at Site 796. A weak opal-A/opal-CT reflector is observed at 0.30 s bsf. The acoustically opaque interval represents abundant input of coarse materials into the sedimentary section. The top of Unit IV makes a strong reflector in correlation with the alternation of tuff and pebbly claystone. The bottom of Hole 796B (465 mbsf) is estimated to be 100 m above the acoustic basement.

Heat Flow and Temperature

Temperature measurements were made using the Uyeda probe at five points down to 127.1 mbsf in Hole 796A and at three points down to 79.8 mbsf in Hole 796B. The measurements in Hole 796A yielded spurious data because of an encounter with coarse sediments at several points. The measurements in Hole 796B yielded valid data with a temperature gradient of 178°C/km and a heat-flow value of 156 mW/m², the highest heat flow that has ever been measured in the Japan Sea. Preliminary calculation shows that neither topographic effects nor frictional heating along thrust faults can account for this high heat flow.

Logging and Physical Properties

Four successful logging runs were completed between 100 and 340 mbsf in Hole 796B (combination sonic/lithodensity/temperature/DIT, geochemical, FMS, and BHTV). Resistivity, velocity, and bulk-density profiles characterize the sedimentary section well. As the total recovery of cores is poor at this site, the logging data represent indispensable data needed to complete the description of the lithologic column. The opal-A/opal-CT transition is recognized at 215 mbsf on logs, different from the depth of identification by XRD analyses (225 mbsf). This difference may come from poor recovery from the corresponding zones, and logging data may provide a better estimate of the level of this transition. Sand beds and tuff beds are well identified by the resistivity, velocity, and bulk-density profiles. The FMS data display numerous, mostly horizontal layers with thicknesses ranging from 5 to 30 cm. A BHTV run was executed in the sediment section because some sandstone layers have high sonic velocity (>4000 m/s). Some small-scale fractures were observed but no prominent breakouts were visible on the preliminary BHTV images. Most of the physical properties show variations correlated to lithologic changes.

Site 797

Principal Results

Site 797 is located in the southwestern Yamato Basin at the base of the slope leading to the Yamato Rise and Kita-Okai Bank. The objectives of this site were to (1) determine the age and nature of acoustic basement, (2) measure the direction and magnitude of the present stress field, and (3) characterize the sedimentation, subsidence, and oceanographic evolution of the area.

The principal results at Site 797 were as follows:

1. Acoustic basement at this site comprises basalts and dolerites and interlayered volcanoclastic sandstones, siltstones, and silty claystones. The age of the sediments which overlie the shallowest

basalt layer is 19 Ma. Based on paleodepth estimates using microfossils within these sediments and on sedimentary structures within the underlying volcanoclastic sediments, this part of the Yamato Basin probably subsided rapidly during the early Miocene. The uppermost basalts most likely represent submarine lava flows, whereas the bulk of the underlying igneous units are intrusive sills and dikes. Most of these rocks are high-Al basaltic in composition, consistent with generation during the original stages of arc rifting. However, the lowermost dikes and sills are alkali basalts and hawaiites which are unrelated to the overlying basalts and probably derived from a different mantle source.

2. The *in-situ* stress field could not be determined because poor hole conditions precluded packer/hydrofracture tests. A borehole televiwer log over one basalt interval showed fractures but no borehole breakouts for stress directions.

3. The sedimentary and paleontological sequences indicate at least four principal stages in the evolution of this part of the Yamato Basin (1) an early Miocene period of submarine basaltic volcanism and concomitant deposition of gravity-flow and current-reworked volcanoclastic sandstones and siltstones on a shelf or slope, probably outboard of a delta, (2) a late early to early middle Miocene phase of diminishing submarine volcanic activity, warm surface waters, and deposition of calcareous and slightly phosphatic hemipelagic claystones at lower bathyal depths (1500-2000 m) in a poorly oxygenated basin, (3) a late Miocene to late Pliocene cooling period initiated by an interval of anomalously slow sedimentation (5 m/m.y.) and characterized by dominant but variable diatomaceous sedimentation at lower bathyal depths (1500-2000 m), and (4) a latest Pliocene to Holocene stage during which diatomaceous sedimentation shut down, volcanic-ash production increased, subsidence continued, and climate oscillated to produce a sequence of interlayered light and dark silty clays having variable organic-carbon contents. In contrast with the more northern sites drilled during Leg 127, the sediments at Site 797 contain more carbonate, suggesting that the site was at or near the CCD throughout much of its sedimentary history. Dissolution of silica is pronounced at this site, and the opal-A/opal-CT and opal-CT/quartz diagenetic transitions are well defined.

Lithology

The sedimentary section cored in Holes 797A, 797B, and 797C consists mostly of lower Miocene to Quaternary fine-grained hemipelagic diatomaceous and terrigenous sediments with minor tuff. The division of units is as follows:

Unit I: (0-119.9 mbsf; 0-2.3Ma). Silty Clay and Clay. The upper 82 m of this unit is color-banded, light and dark silty clay, and clay with minor diatom ooze and scattered thin ash layers. Dark layers are moderately well laminated, decrease with depth, and have common pyrite, diatoms, and organic matter. Light layers are bioturbated or faintly laminated. Subtle size grading occurs in the silty clays. The lower 38 m is similar but with increasing diatom content and bioturbation.

Unit II: (119.9-224.0 mbsf; 2.3-4.9 Ma). Diatom Clay and Clayey Diatom Ooze. A high diatom content characterizes this unit, which consists of diatom clay and ooze. All lithologies are extensively bioturbated. Minor dolomitic zones and nodules and some ash occur.

- Unit III: (224.0-301.5 mbsf; 4.9-6.4 Ma). Diatom Clay and Silty Claystone. This unit is mostly bioturbated to indistinctly mottled diatom clay and silty claystone with scattered thin layers of bioclastic sand, minor ash, and carbonate layers and nodules. Faint to distinct light and dark color banding is common. Sands contain foraminifers, sponge spicules, quartz and feldspar. The opal-CT occurs at 290 mbsf. Sponge spicules increase and diatoms decrease downsection.
- Unit IV: (301.5-426.6 mbsf; 6.4-13.7 Ma). Claystone, Silty Claystone, and Siliceous Claystone. Claystone and siliceous claystone characterize this unit. The upper 48.5 m consists of indistinctly color-banded layers. Dark layers are faintly laminated to slightly bioturbated; light layers are moderately to extensively bioturbated and characterized by compacted, horizontal burrows. Secondary carbonate layers are common. Chert occurs rarely. The lower 76.6 m is interbedded claystone, siliceous claystone, porcellanite, and chert which are moderately to extensively bioturbated. Chert is common. One thin, carbonate-cemented, lithic sandstone layer occurs in this interval. The sandstone is normally graded and contains faint laminations.
- Unit V: (426.6-627.3 mbsf; 13.7-19.0+ Ma). Claystone and Tuff. This unit consists mostly of faintly laminated claystone with numerous horizontal, compacted burrows. The claystone is slightly siliceous near the top of the unit but becomes hard and carbonate-cemented at the base. Small, vertically anastomosing, clay-filled fractures are common in the claystone. Stringers and small nodules of secondary carbonate, pyrite, and thin glauconitic layers are also present. Altered tuff layers, up to 10 cm thick, and rare layers of tuffaceous sandstone occur throughout the unit. The lower 73 m of this unit contains interbedded basalts. The sediments of this part of the unit are claystones similar to those above and thin conglomerates composed of entirely of porcellanite pebbles in a siliceous claystone matrix. (Igneous rocks are present below Unit V to 646.9 mbsf.)
- Unit VI: (646.9-900.1 mbsf; >19.0 Ma). Sandstone, Siltstone, and Silty Claystone. Interbedded volcanoclastic and carbonaceous siltstone, sandstone, and minor silty claystone characterize the sediments of this unit. These rocks occur in intervals 1-10 m thick which are interbedded with basalts. Planar and cross laminations, normal size grading, scoured surfaces, load structures, fluid-escape features, and extensive grain alteration to clay are common features throughout the sandstones. The siltstones are planar laminated and commonly contain flattened, bedding-parallel lenses of darker siltstone which may variously represent burrows and rip-up clasts. Rare primary dips and associated small-scale slump structures are present.

Age and Sedimentation Rates

Sedimentation rates are well constrained by diatom zones and to a lesser degree by paleomagnetism in Units I through III (0-301 mbsf). Below this level, all diatoms have been dissolved except those protected in calcareous concretions. Units IV, V, and VI are dated using these sporadic samples together with sparse control from foraminifers, radiolaria, and calcareous nannofossils. The oldest paleontological control is the middle Miocene calcareous nannofossil zone *Sphenolithus heteromorphus*, which occurs between 436 and 494 mbsf. The age of the sediment which overlies the shallowest basalt unit at 554 mbsf is 19 Ma (19-20 Ma) based on extrapolation of the sedimentation rate calculated using the three deepest nannofossil datums. Using all of the age data, sedimentation rates show three distinct trends: (1) 49 m/m.y. for the Quaternary through

uppermost Miocene clay and silty clay and diatomaceous sediments (0-7.0 Ma); (2) 5 m/m.y. for the upper Miocene to upper middle Miocene siliceous claystones, cherts, and porcellanites (7.0-11.6 Ma), and (3) 30 m/m.y. for the middle and lower Miocene claystone, siliceous claystone, and minor tuffs overlying the basalts (11.6-19.0 Ma). Because of the lack of microfossil control, the sedimentation rate for the underlying volcanoclastic sandstones, siltstones, and silty claystones that are interbedded with the basalts is unknown.

Geochemistry

The sediments from Site 797 are characterized by an increase in diagenetic silica below about 300 mbsf and by moderate but variable amounts of organic carbon (TOC; range 0.2-8.5%, average 1.0%) and carbonate. Diatoms and dissolved silica contents of interstitial waters decrease markedly below about 300 mbsf. This diagenetic boundary restricts fluid communication and divides the sedimentary section into upper and lower diffusive regimes. Carbonate values are generally less than 5% below about 300 mbsf, but intervals having 5 to 20% CaCO₃ against a very low background level occur above this depth. The organic-carbon content fluctuates between high and low values coincident with dark and light interlayering in the Quaternary and uppermost Pliocene sediments. Organic-carbon values are also high in the uppermost Miocene diatomaceous sediments (290-330 mbsf). Organic matter is derived from both terrestrial and algal sources. Sulfate is present throughout the section and reflects variations in the sedimentation rates and organic matter. Sulfate shows two peaks, one near the seafloor and a smaller peak at 350 mbsf. Small amounts of methane (3-200 ppm) occurred with only traces of ethane and propane, but no safety problems related to gas were encountered.

Igneous Rocks

Basalt, alkali basalt, hawaiite, and dolerite interlayered with sediments represent acoustic basement cored in Hole 797C. These igneous rocks describe two broad and overlapping groups containing 21 separate units, which are defined on the basis of contact relations, intervening sedimentary rocks, composition, and texture.

Group 1: Units 1, 2, and 4 (553.5-579.5 mbsf; 608.8-609.4 mbsf). These rocks consist of aphyric and sparsely plagioclase olivine phyric basalts interbedded with conglomerate and tuffaceous claystone of sedimentary Unit V. Their brecciated and highly fractured nature, relatively fine grain size, and lack of chilled margins indicate that they most likely represent submarine lava flows. Unit 1 consists of a loose breccia with intercalated clasts of conglomerate, and is perhaps a talus deposit. Units 1 and 2 are petrographically and compositionally similar, although highly altered, and may have erupted during the same effusive episode.

Group 2: Units 3 and 5 through 21 (580.2-608.6; 618.0-900.1 mbsf). The igneous rocks of this group consist of typically highly altered aphyric and sparsely plagioclase phyric basalt and dolerite interlayered with laminated sandstones, siltstones, and claystones of sedimentary Units VI and tuffaceous claystones of sedimentary Unit V. Some of the basalts are only slightly to moderately altered. Their massive nature, relatively coarse grain size, and chilled borders, the latter often associated with baked or alteration margins affecting both the basalts and sediments, indicate that they represent intrusive sills and dikes.

Most of the igneous rocks of Hole 797C are nonvesicular high-alumina basalts and dolerites with low amounts of the large ion lithophile elements Rb, Ba, and K, and low amounts of Nb and Ce. Some of these are quite primitive, with several samples having MgO, Cr, and Ni values exceeding 10%, 150 ppm, and 350 ppm, respectively. They are rich in Al_2O_3 , showing no decrease in Al_2O_3 with lowering MgO, and lack an iron-enrichment trend. These two features imply that the nonalkaline samples have relatively high water contents, which caused suppression of plagioclase crystallization. The extremely low Nb contents are consistent with an arc-related origin, but the low incompatible-element contents (with the exception of Sr) indicate that the lavas interacted very little with continental crust.

In contrast, the lowermost analyzed sills and dikes are vesicular alkali basalts and hawaiites, containing large amounts of the high field strength elements Zr, Y, Ti and Nb; high amounts of the alkalis; and high Rb, Ba, and Ce. These two different types of igneous rocks are genetically unrelated, with the alkaline rocks lacking typical arc signatures. The geologic setting of this site and the igneous compositions suggest that these intrusive and extrusive rocks were emplaced and erupted during the rifting apart of a volcanic arc. The relative timing of emplacement of the different compositional suites is unknown.

Seismic Stratigraphy

Six distinct seismic intervals occur at this site. From top to bottom these are (1) an upper weakly stratified interval, (2) a transparent interval, (3) a faintly stratified interval, (4) a well-stratified interval, (5) a lowermost irregularly stratified interval, and (6) an unstratified, acoustically opaque zone. Interval 1 correlates with Unit I. Interval 2 corresponds to Units II and III. Interval 3 correlates with Unit IVA. Interval 4 correlates with Unit IVB and the upper part of Unit V. Interval 5 correlates to the interlayered basalts and sedimentary rocks of Unit V. Acoustic basement, the last interval, correlates to the lowermost part of Unit V and Unit VI and is composed of interlayered basalts, dolerites, and sedimentary rocks. The opal-A/opal-CT diagenetic boundary is in the uppermost part of interval 3. Acoustic basement, consisting of interlayered sedimentary rocks and basalt and dolerite sills and flows, is representative of that of much of the Yamato Basin. Seismic reflection alone cannot address the thickness of this interlayered sequence. This interval may be correlatable to the so-called 3.5 km/s layer of Ludwig et al. (1975), and may have a thickness of 1-2 km in the Yamato Basin.

Heat Flow

Successful temperature measurements were made using the Uyeda probe at six points down to 185.5 mbsf in Hole 797B. The measured gradient is $123^{\circ}C/km$. The calculated heat-flow value using this gradient and measured thermal conductivities is $101 mW/m^2$. This value is identical to a nearby seafloor measurement and similar to the average heat flow for the entire Yamato Basin ($97 \pm 12 mW/m^2$). In contrast, this value is somewhat greater than the local average for this part of the Yamato Basin ($87 mW/m^2$).

Logging and Physical Properties

Successful logging runs were completed in the upper part of Hole 797C between 80 and 516 mbsf in Hole 797C. The combination sonic/lithodensity/temperature/induction string and the FMS were run in open hole over this interval. Below 516 mbsf, logging was restricted by unstable hole conditions caused by rapidly swelling clays in highly altered tuffs and volcanoclastic strata. The geochemical log was run behind pipe from 0 to 633 mbsf, and partial runs were made with the FMS (485-610 mbsf) and the borehole televiewer (549-603 mbsf) using the side-entry sub. The rotatable, single-element packer was in the drill string during the logging runs, but poor hole conditions precluded its use. The logging data above 516 mbsf provide a useful characterization of the sediments, particularly over the chert and porcellanite interval (350-430 mbsf), where core recovery was poor. The geochemical log and the FMS log provided compositional and structural data in the uppermost interbedded basalts and sediments.

The water content of the sediments intercalated with the basalts and dolerites is remarkably low (10-24%), suggesting that there has been some thermal interaction with the igneous rocks. General profiles of the physical properties at Site 797 mimic Site 794 profiles closely, suggesting similar basin-wide processes controlling the sediments and their diagenesis.

CONCLUSIONS

Successful drilling in the Japan Sea during Leg 127 addressed all of the proposed principal objectives. At three of the four drilling sites (Sites 794 and 797 in the Yamato Basin and Site 795 in the Japan Basin) we penetrated and obtained the age of acoustic basement and recovered the complete overlying sedimentary section. At Site 796 on Okushiri Ridge, drilling recovered the upper 80% of the sedimentary column. These data provide unequivocal, crucial information on the geology of this marginal basin, which developed along an active continental margin. The information gathered includes data from a wide variety of geoscience disciplines which can be tied to an equally large data base in the region.

We achieved three of the four principal objectives of our drilling: age and nature of basement, recent convergence tectonics along the eastern margin of the Japan Sea, and the sedimentary and oceanographic evolution of the basins. We were unable to obtain our fourth objective, that of obtaining *in-situ* stress measurements, because of unstable hole conditions at all of the sites. The drilling penetrated acoustic basement of the Japan Sea for the first time, and our program was fully successful in all aspects except for the *in-situ* stress measurements. In the discussion that follows, we summarize the conclusions of Leg 127, focusing on the tectonic, sedimentological, and paleoenvironmental aspects.

Principal Tectonic Aspects of the Results

(1) Age and Nature of Basement

We penetrated acoustic basement at Sites 794, 795, and 797. In the Yamato Basin at Sites 794 and 797, we found that the acoustic basement was composed of interlayered basalts and sediments, but not the true basin basement. At Site 797, we drilled 350 m into this interlayered rock and recovered 21 separate basaltic sills and flows, but still did not reach the basin basement. At Site

794, we encountered 1.5 m of tuff and tuffaceous claystone and basalt beneath 100 m of dolerite sills. In the Japan Basin, we reached acoustic basement at Site 795, but not at Site 796 on Okushiri Ridge. At Site 795, we penetrated 76 m into acoustic basement and recovered basaltic and andesitic brecciated lavas. We may have reached basement at this site, as it is located on a small basement ridge that probably represents a volcanic pile. However, shallow penetration into the acoustic basement at the site does not exclude the possibility that the flows are underlain by sedimentary layers.

Given these findings, we cannot say with confidence that we reached basin basement at any of the sites of Leg 127. In terms of the age constraints of basin formation, however, these drilling results provide high-quality data. At all drilling sites micropaleontological data, specifically rare occurrences of calcareous nannofossils and planktonic foraminifers in the sediments as well as diatoms in dolomite nodules, provided crucial age constraints in the lower part of the sedimentary column. We were able to assign the age of the shallowest sediment/basalt contacts at Sites 794, 795, and 797 according to these paleontological constraints. These are: Site 794, 14.8-16.2 Ma, with the best estimate being 15.5 Ma; Site 795, 13-15 Ma, with the best estimate being 14 Ma; and Site 797, 16-20 Ma, with the best estimate being 19 Ma. Simple extrapolation of the sediment-accumulation curve at Site 796, where drilling was terminated at 110 m above acoustic basement, provides an estimated basement age of 17 Ma.

Among these four sites, the age of the lowest sediments is oldest at Site 797. This finding provides crucial information about the initiation of basin formation of the Japan Sea. The sediments just above the shallowest basalt at this site are phosphatic siliceous claystones; the benthonic foraminiferal assemblage in this claystone indicates a lower bathyal level, suggesting that the basin was already well developed by 19 Ma. As Site 797 is located at the margin of the Yamato Basin, this age provides the first clear evidence that constrains the initial stage of the opening of the Yamato Basin. The younger basal sediment age at Site 794, located at the central part of the Yamato Basin, as well as the forthcoming Ar40-Ar39 absolute age data on the basalts, will constrain the age of the final stage of the Yamato Basin opening.

The age of the bottom of the sedimentary column at Site 795 in the northern margin of the Japan Basin indicates that the volcanic activity occurred at 14 Ma in upper bathyal water depths, and suggests that the volcanic activity in the basin lasted until 14 Ma. We are uncertain as to whether this volcanic activity is correlated to any stage of basin formation. Further detailed seismic stratigraphic study and further geochronological and petrochemical studies of the recovered basaltic rocks will help relate the nature of this basement to other basement in the Japan Basin.

A principal finding of Leg 127 is that the acoustic basement of the Yamato Basin was revealed to be interlayered basalts and sediments. Although this was proposed to some extent from its smooth surface and velocity structure (Ludwig et al., 1975; Tokuyama et al., 1987), identical acoustic basement is probably representative of most acoustic basement of the basinal areas of the Japan Sea based on seismic reflection profiling data and sonobuoy wide-angle reflection data. As the 3.5 km/s layer of the wide-angle reflection data may correlate to this interbedded zone, the thickness of this interbedded interval may be as thick as 0.5-2 km in the basinal area. The recovered interbedded unit, with a thickness much greater than that of seismically visible upper sediments, unequivocally improves the understanding of basinal structure in this marginal basin.

In conclusion, drilling results in the Yamato Basin that penetrated acoustic basement well constrain the age of basin formation, while those of the Japan Basin may partly constrain the age of that basin. The discovery of the nature of acoustic basement in the Yamato Basin revealed by the Leg 127 drilling is a crucial achievement toward improving the understanding of the structure of the Japan Sea basins.

(2) Style and Dynamics of Opening

Some of the most important evidence obtained by our drilling concerning the style and dynamics of the opening of the Japan Sea comes from the lowermost sedimentary sequence interlayered with basalt sills and flows at Site 797. The 350 m of drilling below the shallowest basalt recovered lower Miocene sediments indicative of shallow marine to upper bathyal environments. Currently these rocks occur at depths greater than 3500 m. The lower part of the lower Miocene sequence (lithologic Unit VI) consists of a rhythmical sequence of fine- to coarse-grained sandstones and siltstones containing abundant plant debris. The character of these sediments reflects rapid sediment accumulation. This sequence suggests that the site occupied a marine upper slope proximal to a deltaic depositional environment. In contrast, the upper part of this lower Miocene sequence (lithologic Unit V) consists of laminated claystones intercalated with phosphatic carbonate stringers, suggesting a significantly deepened and widened basinal environment. This influence is well supported by the occurrence of benthonic foraminiferal assemblages indicative of lower bathyal depths. These strikingly different sedimentary facies unequivocally document the rapid subsidence of this part of the basin in the early Miocene (probably before 19 Ma). Our tectonic view of the reconstruction of this sedimentary basin suggests a probable generation of a graben or an initial rift invaded by marine waters some time in the early Miocene and subsequent rapid basin deepening with an approximate rate of 250 m/m.y. by 19 Ma. This rapid subsidence event took place at the basin margin and is apparently coeval with the initiation of the opening of the Yamato Basin.

This rifting and the subsequent subsidence event are associated with abundant volcanic activity, as represented by the basaltic rocks that were recovered at Sites 794 and 797. Determination of the radiometric ages and isotopic compositions of the basalts, together with further petrological and geochemical work, will provide critical information on the dynamic interrelationships between basin formation and magmatism.

The igneous rocks at Site 797 consist of high-Al basalt in the upper part of the interlayered sequence, and alkaline basalts in the lower part. The alkaline basalts may represent volcanism associated with the early rifting of a continental arc, based on analogy with present-day association of similar alkaline basalts with continental rifting. Volcanic activity as represented by the overlying incompatible-element poor, high-Al basalts is consistent with the rifting of a volcanic arc, where the crust has been ruptured and extended sufficiently so that the lavas have interacted little if at all with continental crust. The tholeiitic dolerites of Site 794 are somewhat similar to the high-Al basalts at Site 797, but contain less of an arc signature and more of a mid-ocean-ridge-basalt (MORB) signature in their composition. This compositional difference is consistent with eruption in the center of the Yamato Basin after substantial backarc spreading had occurred. As seismic stratigraphy suggests widespread occurrence of these sills in the entire Yamato Basin, the intrusion

of sills into sediments has played a significant role in the formation of the anomalously thick "oceanic crust" of the Yamato Basin. The subaqueous "blue tuff" beds that were observed at all sites in the middle Miocene sequence may possibly be related to this intense intrusive activity and suggest the occurrence of some submarine volcanoes during the middle Miocene.

Calc-alkaline basalt, basaltic andesite, and basaltic breccia constitute the acoustic basement at Site 795. These lavas share some magmatic compositional affinities with the high-Al basalt at Site 797. This similarity may suggest that the volcanism at Site 795 is also related to the initial stages of arc rifting during initial basin formation. As the estimated age of the Site 795 basalt is 14 Ma, the northernmost part of the Japan Basin may have been initially forming by this time. However, our rather shallow penetration into the basement makes further inferences difficult.

In conclusion, the drilling data suggest that the Yamato Basin formed by the following straightforward model: (1) the initiation of rifting of a continental arc in the middle early Miocene associated with deltaic or shallow marine clastic deposits and alkaline basalt and high-Al basalt volcanic activity, (2) basin deepening and the start of widening of the basin in the late early Miocene associated with rapid subsidence and continuing intrusion and extrusion of high-Al basalts, and (3) continued, constant basin widening and deepening in the late early Miocene and early middle Miocene with frequent tholeiitic dolerite sill intrusions and probable associated submarine volcanism. Nevertheless, the actual mechanism of basin deepening and widening is still unresolved although several possible models may apply. These models include (1) Guaymas Basin style dike/sill intrusions associated with seafloor spreading, where the sedimentation rate is high relative to the volcanism, or (2) ductile continental (arc) crustal extension focused in the lower crust. The formation of the Japan Basin cannot fully be addressed by on-board synthesis and will depend on further synthetic study.

(3) Quaternary Convergence Tectonics along the Eastern Margin of the Japan Sea

The age of the initiation of the uplift of Okushiri Ridge was determined by the shallowest occurrence of a sand bed. The age of the shallowest sand bed is 1.8 Ma, based on its occurrence between the *Actinocyclus oculatus* and *Neodenticulata koizumii* diatom zones. Below this, abundant occurrences of fine- to coarse-grained sand beds (1-10 cm thick) with sharp basal contacts and grading that suggest a turbiditic origin were observed in the upper Pliocene unit as well as in the underlying lower Pliocene to upper Miocene units. These depositional data suggest that turbidites were able to reach Site 796 during this time interval, and that Okushiri Ridge did not yet exist. The shallowest appearance of these sand beds at 1.8 Ma indicates that Okushiri Ridge (WD 2300 m) was uplifted 1300 m above the Japan Basin floor (WD 3600 m) at 1.8 Ma at a rate of 0.7 mm/yr. The seismic stratigraphy at Hole 796A suggests that the unconformity exists at the uppermost Pliocene and that this unconformity broadly extends around the site. This observation further support the uplift of Okushiri Ridge in the latest Pliocene. As the uplift of Okushiri Ridge is caused by thrust activity along the eastern margin of the Japan Sea (a possible new Eurasian-North American plate boundary), these results provide the first exact age data on the initiation of the convergence along this margin and are crucial to address the tectonics of this possible new plate boundary.

The highest heat flow ever obtained in the Japan Sea, 156 mW/m², was measured at Hole 796B. The associated high temperature gradient (178°C/km) is quite consistent with the shallow, obscured opal-A/opal-CT transition zone (215 mbsf, 40°C). Seismic stratigraphy shows that the depth of the opal-A/opal-CT reflector is generally shallower than that of the adjacent Japan Basin itself, suggesting that anomalously high heat flow is widespread over the Okushiri Ridge. Frictional heating along the thrust faults is one potential source of excess heat, but frictional heat alone cannot account for this high heat flow. A mechanism to concentrate the heat flow, such as fluid flow along faults, is required to match the magnitude of the anomaly. The possibility of vertical flux, however, was not confirmed by the geochemical data of interstitial water, physical-property data, and log data, although all of them show many anomalous vertical profiles of elements and physical properties.

Oceanographic and Sedimentation History

In addition to the tectonic findings, Leg 127 also provided valuable new information and insights to the oceanographic and sedimentological development of the Japan Sea from the early Miocene to the present. In the final sections, we briefly consider these findings in terms of two main aspects, paleoenvironment and post-depositional processes.

(1) Paleoenvironments

The vertical and lateral sequence of sedimentary facies encountered at the four drill sites form the basis for our environmental reconstructions of the Japan Sea (Fig. 3). Sites 794, 795, and 797 provide the best hemipelagic records most suitable for this purpose. Site 796 allows a glimpse of the interplay of tectonics and sedimentation along the eastern margin of the Japan Sea.

The environmental changes define at least five distinct periods (A-E in Fig. 3), beginning in the early Miocene. Our earliest record of sedimentation is from the southern Yamato Basin at Site 797. The drilling results revealed that in early Miocene time (E in Fig. 3) this part of the Japan Sea was probably an upper bathyal shelf or slope dominated by clastic sedimentation just outboard or seaward of a delta. The sequence consists principally of graded and current-reworked volcanoclastic sandstones and siltstones containing abundant, terrestrially derived carbonaceous debris. These strata are intercalated with mafic flows, minor breccias, and shallow intrusive rocks and were probably deposited below wave base and coincident with submarine volcanism during a rifting phase of this part of the Japan Sea.

The second period, middle and early late Miocene (D in Fig. 3), was characterized by moderate to rapid subsidence of the Japan and Yamato Basins and deposition of hemipelagic siliceous claystone containing carbonate and phosphatic nodules and lenses, minor glauconite, and low amounts of organic carbon. Benthic foraminifers and the faintly laminated and moderately bioturbated character of these sediments indicate deposition in suboxic waters at depths of approximately 500-1500 m. Slightly greater water depths (2000 m), warmer surface waters, and variable sedimentation rates occurred in the southern Yamato Basin (Site 797) relative to the northern Yamato Basin and Japan Basin (Sites 794 and 795) during this period. Seafloor volcanism persisted as evidenced by the ubiquitous occurrence of gravity-flow tuffs.

The third stage spanned most of the late Miocene and Pliocene (C in Fig. 3) and corresponds to a period of continued subsidence, lowered surface-water temperatures, and moderate to poor oxygenation of deeper waters. The sediments that characterize this period are hemipelagic siliceous claystones and diatomaceous silty clay with variable organic-carbon contents at the basinal sites (Sites 794, 795, and 797), and mixed hemipelagic claystones and massive, gravity-flow pebbly claystones at the marginal site (Site 796). In addition, a significant pulse of organic-carbon input and preservation occurred in the Yamato Basin (Site 794 and 797) during the middle part of the late Miocene. This pulse is not recorded in the Japan Basin sites, suggesting that barriers to circulation may have existed between the two areas at that time. Water depths in both basinal areas ranged from ~1500 to 2500 m.

A Pliocene period (B in Fig. 3) of high productivity, manifested by a distinctive and widespread diatomaceous facies, characterized much of the fourth stage of deposition in the basinal areas of the Japan Sea. Cool surface waters persisted during this period, and sea ice was present at the northern sites (Sites 795 and 796). Along the eastern margin, pulses of volcanoclastic turbidity currents interrupted hemipelagic sedimentation. Subsidence also continued during this time and water depths ranged from 1500 to 3500 m in the northern areas (Sites 757 and 796) and 1500 to 3000 m in the Yamato Basin (Sites 794 and 797).

The latest Pliocene and Quaternary period (A in Fig. 3) brought this sedimentary history to a spectacular finale. At all sites this phase is characterized by a distinctive sequence of interlayered light and dark silty clays punctuated by volcanic ash. Away from these sites, particularly in the deeper parts of the Japan and Yamato basins and in the small coastal basins along northern Honshu, this hemipelagic sequence has been overwhelmed by voluminous input of terrigenous clastic material derived from uplifted terranes in Japan. In the hemipelagic sediments found at the Leg 127 sites, the early Quaternary period is marked by the ubiquitous disappearance of benthic foraminifers, which is suggestive of either widespread and complete dissolution or bottom-water conditions unsuitable for life. In general, the dark layers of the uppermost Pliocene-Quaternary sequence contain more organic carbon and siliceous and calcareous microfossils than the light bands. Both types of layers are variously massive to laminated, and subtle size-grading is common. These characteristics, along with the coeval deposition of coarser clastic material away from the sites, argue for the occurrence of basin-wide oscillations in anoxia and sediment input that ultimately must have been controlled by climate and tectonism. This inference is further supported by distinctive vertical and geographical variations in temperate and subarctic microfossil assemblages which track temporal climatic changes and demonstrate that the northern locations have remained persistently cooler than the southern sites throughout this period.

(2) Post-Depositional Processes

Pronounced overprinting of primary depositional signals by diagenetic processes occurs at all Leg 127 site. The most widespread process affecting the sediments is alteration of opaline diatomaceous sediments to hard porcellanites and siliceous claystones with depth. Two silica transformations accompany the lithologic changes, opal-A to opal-CT and opal-CT to quartz. The opal-A/opal-CT transition is the most conspicuous change, as it affects all physical properties of

the sediments as well as the interstitial-water chemistry; this transition is manifested also in the downhole logs and in all seismic reflection records surrounding the sites as a strong bottom-simulating reflector that locally cuts across reflectors originating from stratal boundaries. The opal-A/opal-CT transition occurs at about 225 mbsf at Site 796 and at approximately 300 mbsf at Sites 794, 795, and 797, corresponding to present subsurface temperatures in the range of 36-55°C. Opal-CT transforms to quartz ~80-150 mbsf below the opal-A/opal-CT transition at all sites, corresponding to temperatures of 49-64°C.

An additional significant post-depositional process at work in the Japan Sea is the biodegradation of organic matter. Organic-matter preservation is rather low in the sedimentary section except for parts of the Quaternary at all sites and the upper Miocene at Sites 794 and 797 in the Yamato Basin. The degree of preservation and the pathways of degradation reflect supply, bottom-water conditions during deposition, and rates of burial. The two sites in the Yamato Basin are characterized by interstitial waters with undepleted sulfate, low amounts of biogenic gas, and low to moderate rates of sedimentation. These trends are generally reversed at the Japan Basin sites, suggesting that sedimentation rates strongly influence the degradational processes affecting organic matter by controlling both the supply of material and the resident time of this material within the subsurface zones of bacterial decay.

These diagenetic transformations are both a hindrance and an aid to the geological interpretations. On the one hand, these processes severely limit our ability to see primary signals. The destruction of the siliceous microfossil record with burial is the best example of this condition. On the other hand, the diagenetic effects provide valuable information on the temperature history of the region. This aspect is extremely valuable at Site 796, where uplift may have caused recent perturbations of the heat flow.

REFERENCES

- Fukao, Y., and Furumoto, M., 1975. Mechanism of large earthquakes along the eastern margin of the Japan Sea. *Tectonophys.*, 25:247-266.
- Gnibidenko, H., 1979. The tectonics of the Japan Sea. *Mar. Geol.*, 32:71-87.
- Ingle, J. C., Jr., 1975. Summary of late Paleogene and Neogene insular stratigraphy, paleobathymetry, and correlation, Philippine Sea and the Sea of Japan. In Karig, D. E., Ingle, J. C., Jr., et al., *Init. Repts. DSDP*, 31: Washington (U.S. Govt. Printing Office), 837-855.
- Ishiwada, Y., Honza, E., and Tamaki, K., 1984. Sedimentary basins of the Japan Sea. *Proc. 27th Internat. Geol. Congress (Paris)*, 23:43-65.
- Karig, D. E., Ingle, J. C., Jr., et al., 1975. *Init. Repts. DSDP*, 31: Washington (U.S. Govt. Printing Office).
- Kimura, G., and Tamaki, K., 1986. Collision, rotation and back-arc spreading in the region of the Okhotsk and Japan Seas. *Tectonics*, 5:389-401.
- Kobayashi, K., 1985. Sea of Japan and Okinawa Trough. In Nairn, A., Stehli, F., and Uyeda, S. (Eds.), *The Ocean Basins and Margins. V. 7a, The Pacific Ocean*: New York (Plenum Press), 419-458.

- Ludwig, W. J., Murauchi, S., and Houtz, R. E., 1975. Sediments and structure of the Japan Sea. *Geol. Soc. Am. Bull.*, 86:651-664.
- Seno, T., and Eguchi, T., 1983. Seismotectonics of the western Pacific region. In Hilde, W.C.T., and Uyeda, S. (Eds.), *Geodynamics of the Western Pacific and Indonesian Regions*. Am. Geophys. Union, Geophys. Monogr., 11:5-40.
- Tamaki, K., 1986. Age estimation of the Japan Sea on the basis of stratigraphy, basement depth and heat flow data. *J. Geomag. Geoelectr.*, 38:427-446.
- _____, 1988. Geological structure of the Sea of Japan and its tectonic implications. *Bull. Geol. Survey Japan*, 39:269-365.
- Tokuyama, H., Suyemasu, M., Tamaki, K., Nishiyama, E.-I., Kuramoto, S.-I., Suyehiro, K., Kinoshita, H., and Taira, A., 1987. Report on DELP1985 cruises in the Japan Sea, Part II: Seismic experiment conducted in the Yamato Basin, Southeast Japan Sea. *Bull. Earthquake Res. Inst. Univ. Tokyo*, 62:347-365.
- Yamazaki, K., Tamura, T., and Kawasaki, I., 1985. Seismogenic stress field of the Japan Sea as derived from shallow and small earthquakes. *Zisin*, 38:541-558 (in Japanese).
- Yoshii, T., and Yamano, M., 1983. Digital heat flow data file around the Japan islands (Ocean Research Institute Files).

FIGURE CAPTIONS

Figure 1. Bathymetric map of the Japan Sea; bathymetric contours are in meters. ODP Leg 127 sites are shown as large dots; DSDP Leg 31 sites are shown as smaller dots. Toothed line represents the Japan Trench.

Figure 2. Map showing major lithospheric plates (A) and microplates (B) in the Japan Sea region. See text for references.

Figure 3. Lithologic summary and correlation of Leg 127 sediments. A to E define common lithofacies between sites. A: Quaternary to Pliocene laminated silty clay. B: Pliocene to upper Miocene bioturbated diatom ooze and diatom clay. C: middle to upper Miocene bioturbated to faintly laminated siliceous claystone and silty claystone, with thin chert layers and minor calcareous layers and nodules. D: middle to upper Miocene tuff and interbedded claystone. E: lower(?) Miocene graded and planar- to cross-laminated, fine-grained sandstone and siltstone interlayered with basalts and dolerites at Sites 794 and 797.

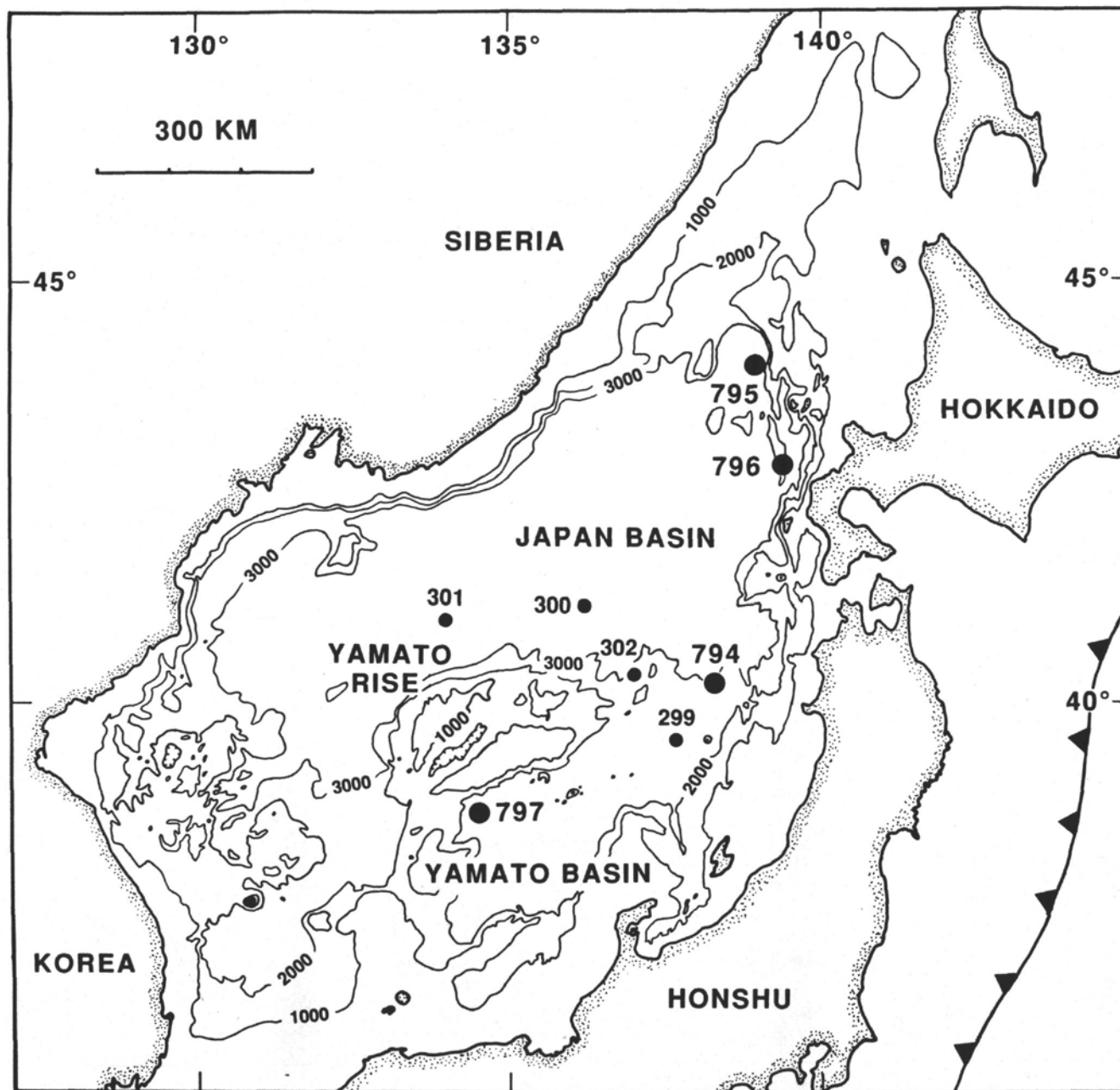


Figure 1. Bathymetric map of the Japan Sea; bathymetric contours are in meters. ODP Leg 127 sites are shown as large dots; DSDP Leg 31 sites are shown as smaller dots. Toothed line represents the Japan Trench.

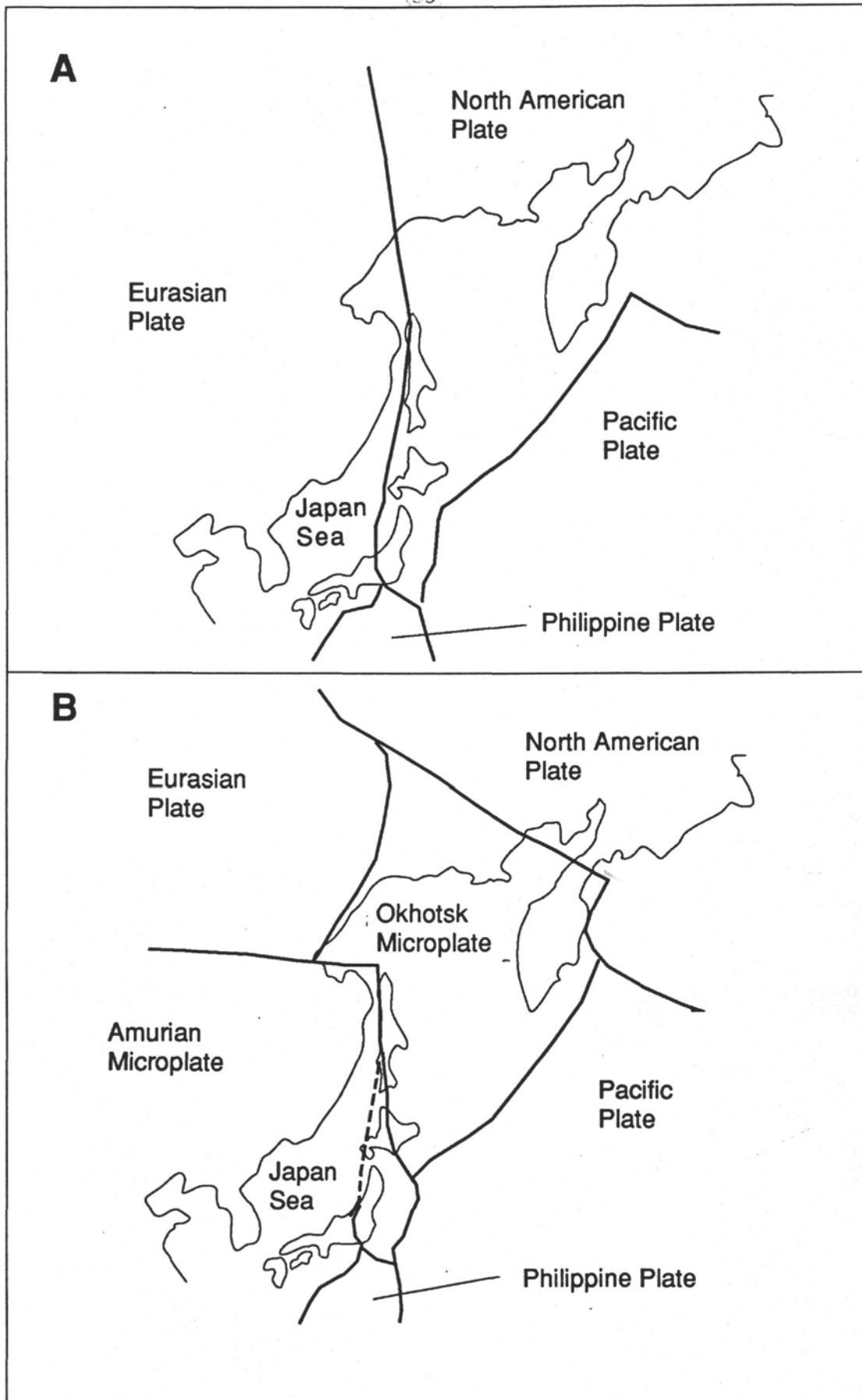


Figure 2. Map showing major lithospheric plates (A) and microplates (B) in the Japan Sea region. See text for references.

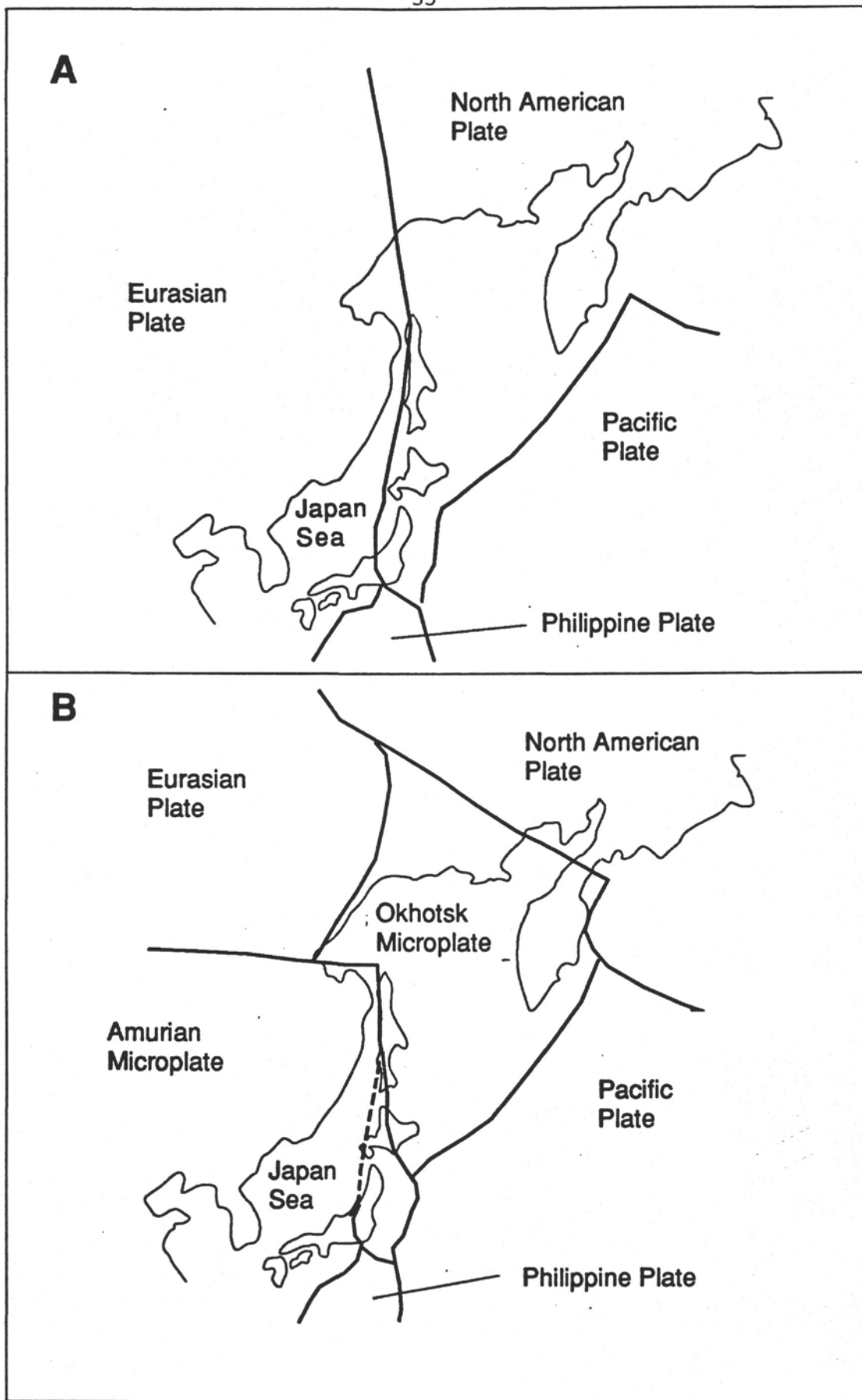


Figure 2. Map showing major lithospheric plates (A) and microplates (B) in the Japan Sea region. See text for references.

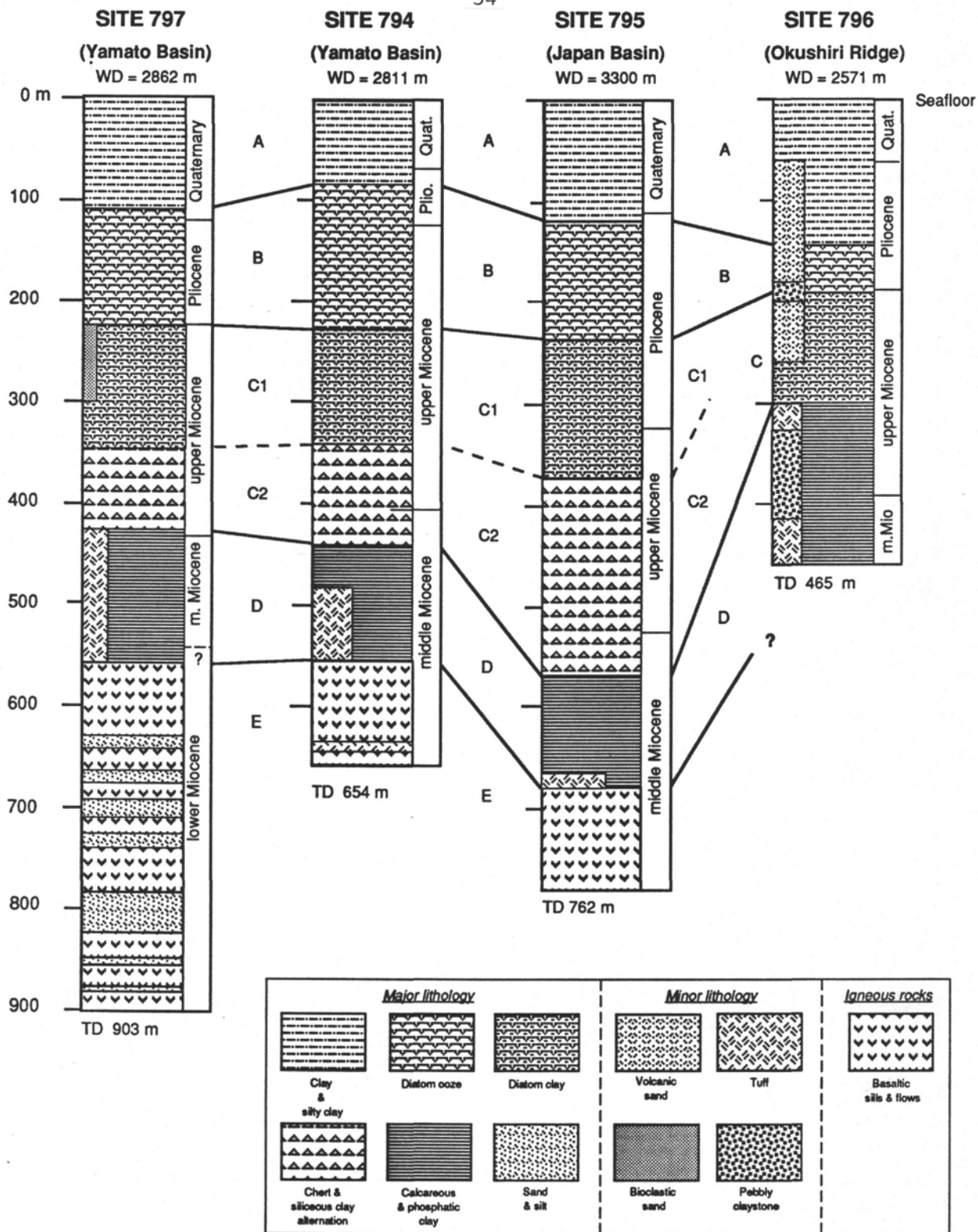


Figure 3. Lithologic summary and correlation of Leg 127 sediments. A to E define common lithofacies between sites. A: Quaternary to Pliocene laminated silty clay. B: Pliocene to upper Miocene bioturbated diatom ooze and diatom clay. C: middle to upper Miocene bioturbated to faintly laminated siliceous claystone and silty claystone, with thin chert layers and minor calcareous layers and nodules. D: middle to upper Miocene tuff and interbedded claystone. E: lower(?) Miocene graded and planar- to cross-laminated, fine-grained sandstone and siltstone interlayered with basalts and dolerites at Sites 794 and 797.

OPERATIONS SYNOPSIS

The ODP Operations and Engineering personnel aboard JOIDES Resolution for Leg 127 were:

Operations Superintendent:	Glen Foss
LDGO Logging Technician:	John Schwartz
Schlumberger Engineer:	Devon Dartnell

OVERVIEW

Four sites were drilled in the Sea of Japan during Leg 127 of the Ocean Drilling Program. Two sites, 794 and 797, were located in the Yamato Basin, and two sites, 795 and 796, were located farther north in the Japan Basin and on Okushiri Ridge, respectively.

The drilling/coring plan was similar at all sites, with hydraulic piston cores (APC) to refusal followed by a limited amount of extended-core-barrel (XCB) coring in the soft to medium sediments. A standard rotary-cored (RCB) hole was then to be drilled through the firmer sediments and into basement. In addition, a third hole with a dual-casing reentry cone installation was planned for Site 794, where an extensive (100 m+) basement penetration was scheduled.

Hole 794A was APC-cored to overpull refusal at 140 mbsf with excellent core recovery and quality. Coring continued with the XCB until hard, siliceous sediments were encountered and was terminated at 351 mbsf. Hole 794B began with a jetting test to determine conductor casing point, then was drilled, with "spot cores," to 338 mbsf. Continuous RCB coring proceeded 6 m into basaltic basement, which was encountered at 543 mbsf, and was terminated at that depth owing to slow penetration. A successful logging program was carried out. A full reentry cone assembly, with 16-in. casing to 80 mbsf and 11-3/4-in. casing to 517 mbsf, was installed in Hole 794C. After a basement penetration of 111 m, the drill string became stuck and could not be freed. A back-off operation was conducted, and the hole was abandoned pending fishing operations with special equipment on Leg 128.

At Site 795, the initial hole was cored to refusal at 172 mbsf with the APC, again with excellent results. XCB refusal again came in siliceous claystones at 366 mbsf. Spudding of Hole 795B was delayed when the lower one-third of the drill string was lost to a pipe failure during the trip to the seafloor. With a replacement bottom-hole assembly (BHA), the hole was drilled to 365 mbsf before RCB coring began. The bit reached basement at 685 mbsf, and coring was terminated at 762 mbsf. Deteriorating hole conditions limited logging operations to the upper 220 m of the hole.

Hole 796A encountered difficult conditions that stopped APC coring at 59 mbsf owing to dolomite concretions. The XCB encountered loose, coarse sands, gassy sediments, and gas hydrates at shallow depths, but then enjoyed more success until siliceous sediments effected refusal at 243 mbsf. Hole 796B was drilled at an offset location and avoided the loose sands. Several shallow spot cores were taken, and the hole was drilled to 243 mbsf for the start of continuous RCB coring. Tight-hole conditions stopped penetration at 465 mbsf, short of basement. Logs were recorded only above 329 mbsf.

Hole 797A was a "false start," consisting of a single APC core taken from below the seafloor. APC cores in 797B continued to refusal at 176 mbsf. The XCB system was then "pushed" through the ubiquitous siliceous claystone interval and into the lower claystones to 496 mbsf, where sedimentary rocks became too hard. Because time had been gained through the premature termination of earlier sites, Hole 797C became a reentry hole with a deep basement penetration objective. A reentry cone with 80 m of 16-in. casing was set,

and a 9-7/8-in. hole was drilled to 484 mbsf, where continuous RCB coring began. Basalt was encountered at 554 mbsf, and coring continued with minor hole problems to 800 mbsf. Increasing hole trouble then limited the logging program to a maximum depth of 630 mbsf. Coring continued for an additional 103 m in very poor hole conditions until a pipe twistoff finished drill-string operations for the leg.

Operational achievements of Leg 127 included superb APC results (recovery, quality and orientation) at Sites 794, 795 and 797; successful and extensive temperature profiles at all sites with the WSTP probe; and testing of the sonic core monitor and penetration of 349 m of basalt/sediment "basement" in Hole 797C under abysmal hole conditions.

TOKYO PORT CALL

Leg 127 began with the first mooring line at Harumi Dock, Port of Tokyo, at 2200UTC 18 June 1989.¹ The port call comprised generally routine crew-change and resupply activities. Difficulties were experienced in clearing some high-technology items through Japanese Customs, but all freight items were eventually cleared and loaded, including positioning beacons and pipe-severing explosives. Work items of operational significance were repairing coaxial cable used in reentry operations, loading 100 joints of new 11-3/4-in. casing and loading 355,000 gal of fuel. A logging cable belonging to the Ocean Research Institute was onloaded for use during Leg 128. Training sessions were held for oncoming personnel on the TAM straddle packer and the sonic core-monitoring device. With scheduled activities complete, the vessel departed Tokyo at 0700UTC 23 June.

SITE 794--NORTHEAST YAMATO BASIN

Proposed site J1b-1 was located about 90 nmi west-northwest of the port of Akita on the northwestern Honshu coast. A positioning beacon was launched after a brief survey of the site at 0615UTC 26 June.

Hole 794A

Calm weather provided excellent APC-coring conditions, and continuous APC cores were taken to refusal at 140 mbsf. Core recovery and quality were superb. The cores were oriented beginning with core 127-794A-2H, and WSTP (water sampler, temperature probe) runs were made after each third core.

Continuous XCB coring then proceeded. Water sampling was discontinued, but temperature probe deployments continued each third core to total depth. Core recovery was very good, but decreased somewhat with depth after the siliceous sediment became partially indurated. The final core was taken to 351.3 mbsf and was followed by a temperature probe run.

¹All times given are Universal Time, Coordinated (UTC), formerly Greenwich Mean Time.

Hole 794B

Following the pipe trip, Hole 794B was spudded at 1045UTC 29 June. The bit was jetted into the sediment without rotation to determine the setting depth of the conductor casing. The soft silty clay jetted easily, and the test was discontinued at 100 mbsf.

The hole was drilled, with four "spot cores," to 338 mbsf, where continuous coring began. Hole 794A had bottomed in an interval of transition from soft diatomaceous clay to silicified and indurated claystones. The new lithology manifested itself in a sharply reduced rate of penetration (ROP) and core recovery. The recovery rate increased somewhat with depth, as the claystone became less siliceous and volcanogenic components increased.

Basement rocks were contacted at 543 mbsf. The dense, fine-grained basalt cored at only ~1m/hr. Intentions to core 25-40 m into basement were abandoned owing to the slow progress after 6 m, and coring was terminated at 549 mbsf.

The hole was then conditioned and filled with potassium chloride-inhibited drilling mud, and the drill string was pulled to logging depth at 101 mbsf. Successful logs were recorded with the "quad combo," geochemical, and formation microscanner tools from ~8 m above total depth.

The drill string was recovered and preparations for deployment of the reentry cone began.

Hole 794C

A reentry cone and seven joints of 16-in. conductor casing were made up, connected to the BHA and run to the seafloor. Hole 794C was spudded at 0645UTC 4 July, and the jetting-in operation commenced. The double-jay running tool released prematurely when the casing shoe had reached 80 mbsf, about 10 m short of the intended depth. The cone/casing assembly was reengaged, but no further jetting progress could be made, and the reentry cone was left standing about 10 m above the seafloor.

After the cone/casing had been released, good progress was made in drilling the 14-3/4-in. hole for the surface casing string. Basement (hard drilling) was reached at 512 mbsf (by driller's pipe tally) in only 9-1/2 hr. After 16 m of basement had been drilled, a round trip was made for the 11-3/4-in. casing string.

The surface casing, consisting of 41 joints of 11-3/4-in. casing, was then assembled and run in to reentry depth with the drill string. The reentry was routine, and no impediment was encountered as the casing was run into the hole and landed with the shoe at 3339 m by pipe tally, a depth calculated to put it 6 m below the basalt/sediment interface. The casing string was then released at the hex kelly running tool by turning the drill string to the right. The casing was cemented into place, and another round trip was made for an RCB bit and BHA.

The second reentry was again routine and well centered. The cement, plug, and shoe were drilled out, and the bit broke through into open rathole below the casing shoe at the driller's depth of 3337 m. When the bottom of the hole was finally tagged at 3379.7 m, 30 m deeper than the earlier depth figure, it was evident that there had been a pipe error of one full stand. That meant that the casing shoe had been set 26 m above the igneous contact.

Continuous RCB coring then began. The rock was massive, altered and highly fractured dolerite. ROP ranged from 1 to 4 m/hr, and recovery was fair to poor. Just a few meters above the final target depth, a sudden jump in the circulating pressure forced the slightly premature cessation of coring operations. Two joints of pipe had been pulled, beginning the round trip, when the drill string became firmly stuck without warning.

Attempts to jar the BHA free were unsuccessful because the jars could not be actuated-- either because the stuck point was above the jars or the jars were not functional, and 5-1/2 hr of attempting to work the pipe loose failed to dislodge it. It was necessary to run the Schlumberger "string shot" tool and to perform a back-off operation, leaving the BHA in the hole pending fishing operations on Leg 128.

SITE 795--NORTHERN JAPAN BASIN

The second site was located about 220 nmi to the north, nearly midway between the Hokkaido and Siberian coasts. The nearest land was the Syakotan Peninsula, about 80 nmi to the southeast on Hokkaido. The positioning beacon was launched at 1115UTC 12 July.

Hole 795A

APC coring produced generally excellent results from the seafloor at 3311 m to refusal at 172 mbsf. Cores were oriented beginning with 127-795A-2H, and six temperature probe runs were made, all but one of which provided good data.

XCB coring then continued with good recovery until the opal-A/opal-CT boundary in the diatomaceous sediment was reached. Below that depth, hard, porcellanitic material was interspersed with siliceous claystone. Recovery and penetration rates dropped sharply and, after four cores, it clearly was time to make the planned round trip for the RCB system to finish coring the lower sediment section and into basement.

Hole 795B

A new RCB bit and BHA were made up for the trip. As the 71st stand of drill pipe was being lowered to the dual elevator stool on the rig floor, the vessel lurched, and the driller noted a sudden string weight loss of about 100,000 lb. A quick calculation showed this to be the loss of approximately the lower 1000 m of the drill string. The remainder of the drill pipe was recovered, and the break was found to be an apparent fatigue failure in the pin connection of the top joint of the 44th stand of 5-in. drill pipe. The BHA and 131 joints of drill pipe below that point had been dropped to the seafloor.

A complete and essentially identical new BHA was made up, and the vessel was offset 186 m to the west-northwest to minimize risk of encountering the drill string wreckage. Hole 795B was spudded at 0945UTC 16 July. The hole was drilled to 365 mbsf before continuous coring began.

Core 127-795B-2R was being recovered when the rig suffered a total power blackout caused by a transformer fire in one of the silicon control rectifiers. While the fire was being brought under control, no power was available to the thrusters or main shafts for 16 min.

During that time the vessel drifted only 122 m, or 3.7% of water depth, and serious damage to or loss of the drill string was averted only because of the almost total absence of wind or current forces at the time.

Continuous coring then continued with relatively low ROP and very low core recovery through an interval of brittle siliceous claystone. As at Site 794, penetration and recovery rates increased in less siliceous claystones below the problem interval. Volcanic components in the sediments increased with depth, and basement rocks were encountered at about 685 mbsf.

The basement was heterogeneous and highly altered. Average ROP was nearly 8 m/hr, but core recovery was fair to poor owing to crumbling, fracturing and jamming of the material. Some minor hole problems were experienced during the basement drilling. At a total depth of 4072 m (762 mbsf), the drilling objectives were considered fulfilled, and coring was terminated at the request of the scientists.

Serious hole trouble, in the form of pipe-sticking, began as attempts were being made to condition the hole for logging and to fill it with KCl mud.

The first intended log was the LDGO magnetic susceptibility log. On final preparation, the tool would not calibrate and had to be set aside in favor of the LDGO borehole televiwer (BHTV). The light-weight BHTV tool came to rest on an obstruction or restriction in the hole at 221 mbsf and could not be worked past it. The BHTV was recovered, and the drill string was lowered to open the hole and then brought back up to logging depth.

For the next attempt, the much heavier Schlumberger "quad combo" tool string was assembled. It was hoped that its greater momentum would carry it through the recently reopened tight-hole interval. The big tool came to a stop at 218 mbsf, however, and could not be worked deeper. A quad-combo log was recorded through the upper sediment section up to the pipe, and the tool was recovered for another cleanout run with the drill string. Hole conditions had deteriorated badly, however, and the pipe could not be worked past 279 mbsf, where the hole had packed off tightly around the pipe. Logging attempts were discontinued, and the hole was abandoned.

SITE 796--OKUSHIRI RIDGE

The new drill site was located about 70 nmi southeast of Site 795 and just 23 nmi northwest of the westward bulge of Hokkaido's Oshima Peninsula. The volcanic mountains of the peninsula were in plain sight of the drilling location.

Hole 796A

After the drill string had been lowered to "feel for bottom," the first core recovered the sediment/water contact from 2581.8 m. The upper sediment section at Site 796 was not well suited to APC coring. Beginning with Core 127-796A-2H, the cores contained large and numerous gas-expansion voids that disrupted sedimentary structures and thwarted

magnetic orientation efforts. Beginning with Core 127-796A-3H, incomplete stroke was achieved on some cores, and three cutter shoes were ruined by hard strata that later were identified as dolomite concentrations. APC coring was terminated at 59 mbsf after eight attempted cores.

At about the same time the coring mode was switched to XCB, coarse sand strata were encountered that reduced core recovery, caused hole-cleaning problems, and interfered with temperature probe operations. XCB coring continued, however, with large quantities of gas and "live" gas hydrates in the cores. The quantity of gas began to decrease with depth below about 100 mbsf and had dwindled to a mere trace by the calculated base of the hydrate-stable zone at about 220 mbsf. Hole conditions and core recovery also improved with depth for a time, but the hole began to deteriorate below about 200 mbsf. Shortly thereafter, the opal-A/opal-CT boundary was reached, and ROP and core recovery fell sharply in siliceous claystones. Operations in Hole 796A were then terminated at 243 mbsf for the switch to RCB coring.

Temperature probe measurements were again successful in obtaining a profile.

The hole was filled with barite-weighted mud upon abandonment, and the drill string was tripped for the RCB BHA.

Hole 796B

A maximum positioning offset of 250 m east from Hole 796A was made in an attempt to avoid sand-filled distributary channels and to position farther off basement structure for hydrocarbon safety.

Following a mud-line core, the hole was drilled to 30 mbsf. Continuous RCB cores were then taken to 98 mbsf, with successful temperature probe runs at 60 and 79 mbsf. Dolomite nodules again interfered with core recovery, but the relocation apparently was successful in avoiding the main sand bodies, as only a few thin, fine sand strata were encountered. Considerable gas was again found in the shallow cores.

RCB coring resumed after the hole had been drilled to 243 mbsf, the total depth of Hole 796A. Core recovery again was low in the brittle siliceous claystones. Increased friable sand strata and dolomite nodules over the previous two sites did nothing to improve the recovery situation. Gas quantity remained extremely low, with only "background" traces. Real hole-cleaning problems began below about 330 mbsf in fractured pebbly mudstones, and another wiper trip was made from 387 mbsf.

Core recovery then improved considerably in more homogeneous and less fractured siliceous and tuffaceous claystones, but hole conditions began to deteriorate with depth despite mud flushes and elevated circulating rates. At 465 mbsf, another short trip was made in an attempt to clean the hole, but the bit could not be worked past a tight spot at 381 mbsf. It became apparent that further coring in 796B was not feasible.

Despite extensive hole-conditioning efforts and special logging mud mixed to 3.5% KCl concentration above the seawater equivalent, logging tools could not pass an obstruction at about 329 mbsf. Logs recorded were seismic stratigraphy, formation microscanner, geochemical combination, litho-porosity combination, and borehole

televiwer. All reached the same depth, and none found any resistance in the hole.

SITE 797--WESTERN YAMATO BASIN

The new drill site was located well out into the broadest part of the Sea of Japan, about 130 nmi northwest of Honshu's Noto Peninsula. The positioning beacon was dropped at 0230UTC 31 July.

Hole 797A

The drill bit was positioned for the initial APC core at 2877 m. The core barrel was recovered completely full of sediment, indicating that the bit had been below the seafloor at the time of spud. As recovery of the sediment/water interface was critical in determining water depth, the bit was raised to 2870 m for a second attempt.

Hole 797B

The second core barrel recovered the interface and established seafloor depth as 2873.6 m below driller's datum. With the seafloor depth known, a jet-in test to determine the casing point was conducted next. The bit was jetted to 100 mbsf without significant difficulty.

Oriented APC cores were taken with excellent results from the depth of Core 127-797B-1H to refusal at 176 mbsf. Six temperature probe runs were made within the interval.

XCB coring then continued with generally good recovery until hole-cleaning problems developed at about 331 mbsf. A short trip was necessary to clean up the hole. Good core recovery and ROP continued to about 360 mbsf, where the hard, brittle siliceous sediment section found at Sites 794-796 was again encountered. This normally would have been the end of XCB-coring attempts. The XCB was pushed beyond the usual prudent refusal point in Hole 797B because the deepest possible exploratory hole was desired for the planned reentry penetration, and because the hard sediments were a good test for the relatively new XCB-121 system, the PDC bit, and the SCM system.

Around 440 mbsf the porcellanitic sediments gave way to claystone. Core recovery through this interval was somewhat higher than with the RCB, but the ROP was lower. At about 490 mbsf, hard, carbonate-cemented strata were encountered that brought penetration nearly to a halt, and coring was terminated at 496 mbsf owing to the slow progress.

Hole 797C

Seven joints of 16-in. range-3 casing were then made up and landed in a reentry cone. The RCB BHA, casing string and reentry cone were latched together for the pipe trip.

Hole 797C was spudded at 1030 hr, 5 August, on a 30-m southeast offset from Hole 797B. The jetting operation proceeded without undue difficulty, and the casing was released routinely. A round trip and reentry were then required to remove the running tool and latch sleeve from the BHA owing to dimensional incompatibility between the new 8-1/2-in. drill collar in the upper BHA and the latch sleeve of the casing running tool.

Drilling then continued at a good pace. One precautionary wireline trip was made to retrieve the "wash" inner barrel and take a deviation survey at 414 mbsf when the siliceous claystone interval had been partially penetrated. At 484 mbsf, the wash barrel again was recovered, and continuous RCB coring began. Core recovery in the lower sediment section was only fair, but ROP was high. Igneous rocks were encountered at 554 mbsf. Minor hole problems began after only about 35 m of basement penetration. The basaltic rocks became increasingly interbedded with argillaceous siltstone and sandstone sediments with depth. Hole problems began to increase correspondingly until a "short trip" was made after 676 m penetration. Coring then continued, with only minor hole-cleaning problems, to 800 mbsf, where a round trip was made on the basis of bit rotating hours.

The outer core barrel assembly was exchanged for the TAM drilling packer (TDP), and the hole was reentered for logging. With the pipe at casing shoe depth, the FMS and "quad combo" logs were recorded from a bridge in the hole at 516 mbsf.

Next the drill string was run back into the hole to open the way for deeper logging, but the pipe came to a stop on an obstruction at 643 mbsf. The top drive was then picked up, and the hole was reamed and cleaned to just off total depth, where it was again flushed with mud before the end of the pipe was withdrawn to 543 mbsf.

Attempts to log open hole beyond that depth met with little success. The pipe was then washed down to 638 m, a through-pipe geochemistry log was run from there to seafloor depth, and the end of the pipe was raised to 494 mbsf where the side-entry sub (SES) was installed. With the aid of the SES, an FMS log was tied into the log of the upper hole, and a successful borehole televiewer run was made in the upper basalt/sediment interval.

Though a suitable interval for packer permeability tests had been identified around 588 mbsf on the basis of caliper and BHTV logs, it was necessary to cancel the planned packer permeability tests owing to adverse hole conditions.

An additional 103 m of intercalated basalt and claystone/siltstone/sandstone sediment eventually were cored in the next four days. Extremely difficult hole conditions forced several wiper trips to relieve torque, drag and excessive circulating pressure. A round trip and reentry were necessary to remove an obstruction from the core bit, which turned out to be several pieces of basalt core.

On the morning of 18 August, while coring was in progress, the drill pipe parted about 400 m above the bit, effectively ending Hole 797B and Leg 127. The bad hole conditions and only one day of remaining operating time eliminated the possibility of fishing for the BHA.

The next 21 hr was spent in surveying a series of cross-lines in the area of Site 797. At 0445UTC 19 August, *JOIDES Resolution* departed the operating area and steamed toward Pusan, South Korea.

Leg 127 came to its official end when the anchor was let go at quarantine anchorage at Pusan Harbor at 0600 hr, 20 August 1989.

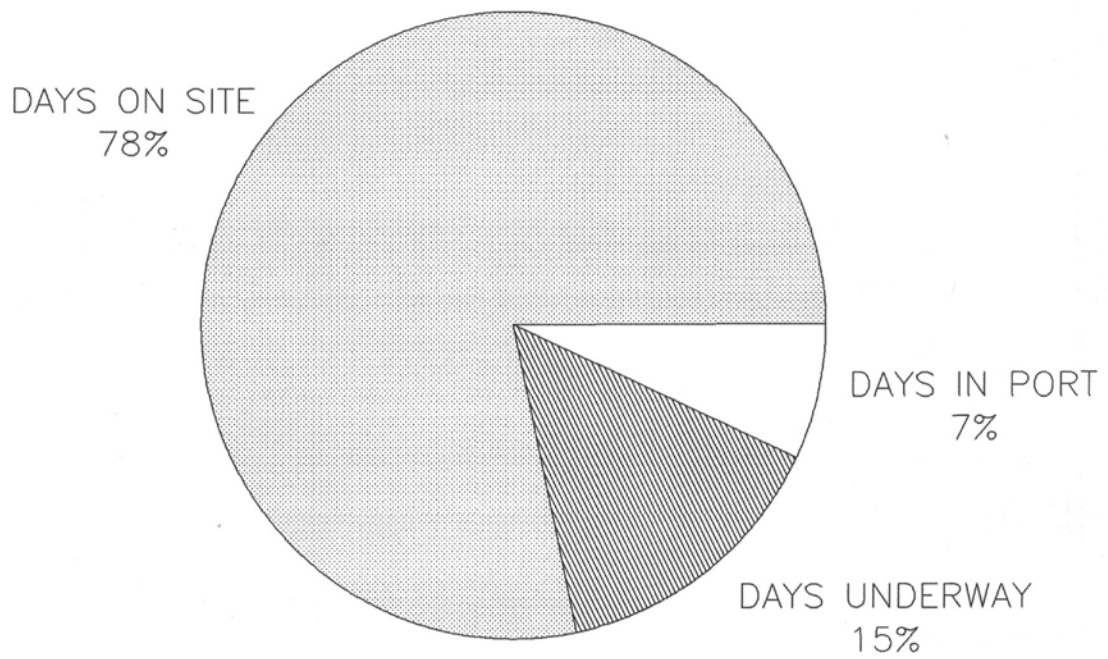
OCEAN DRILLING PROGRAM
 SITE SUMMARY REPORT
 LEG 127

HOLE	LATITUDE	LONGITUDE	DEPTH METERS	NUMBER OF CORES	METERS CORED	METERS RECOVERED	PERCENT RECOVERED	METERS DRILLED	TOTAL PENETRATION	TIME ON HOLE	TIME ON SITE
794A	40-11.41N	138-13.86E	2821.7	37	351.3	302.2	86.0	.0	351.3	69.00	
794B	40-11.40N	138-13.87E	2821.7	27	249.2	87.4	35.0	299.8	549.0	104.25	
794C	40-11.40N	138-13.86E	2820.0	14	93.9	33.2	35.3	559.8	653.7	182.50	355.75
795A	43-59.23N	138-58.03E	3311.2	39	364.9	258.3	70.7	1.0	365.9	757.50	
795B	43-59.24N	138-57.89E	3310.0	41	397.0	188.9	47.5	365.2	762.2	146.75	222.50
796A	42-50.93N	139-24.67E	2581.8	27	242.9	155.3	63.9	.0	242.9	49.75	
796B	42-50.92N	139-24.85E	2633.8	33	293.8	85.3	29.0	171.1	464.9	117.50	167.25
797A	38-36.94N	134-32.16E	2873.6	1	9.5	9.7	102.1	3.4	12.9	8.00	
797B	38-36.94N	134-32.16E	2873.6	53	495.7	370.7	74.7	.0	495.7	94.00	
797C	38-36.93N	134-32.18E	2876.0	46	419.0	164.2	39.1	484.0	903.0	336.00	438.00
TOTALS:				318	2917.2	1655.2	56.7	1884.3	4801.5		1183.50

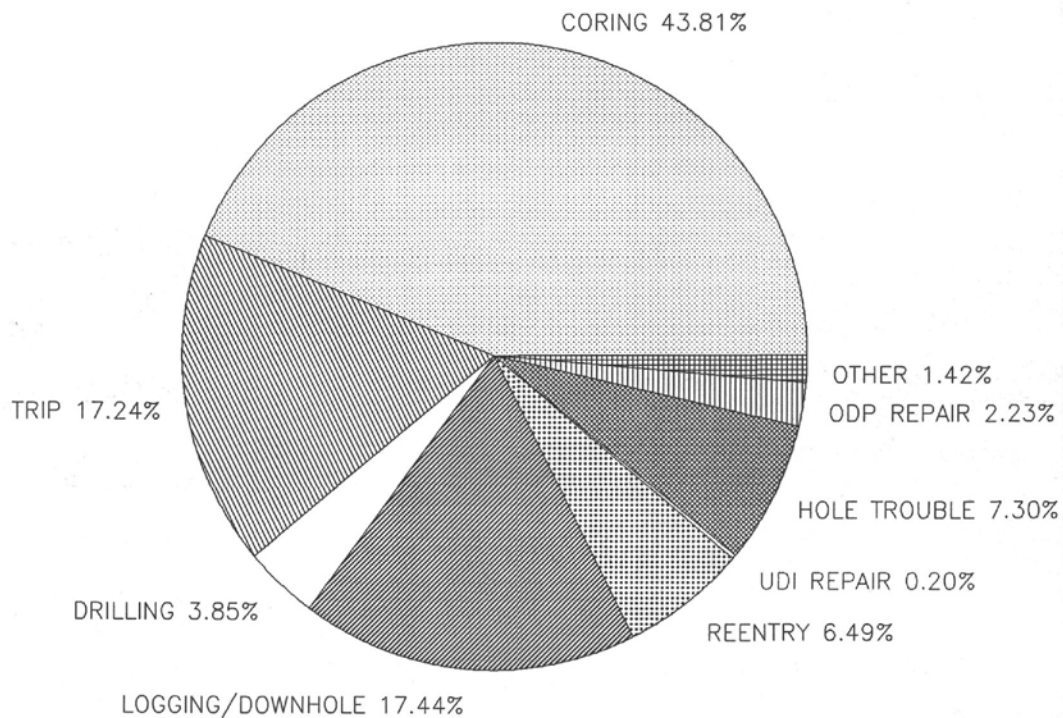
OCEAN DRILLING PROGRAM
OPERATIONS RESUME
LEG 127

Total Days (19 June 1989 - 21 August 1989)	63.0
Total Days in Port	4.4
Total Days Under Way	9.3
Total Days on Site	49.3
Trip Time	8.5
Coring Time	21.6
Drilling Time	1.9
Logging/Downhole Science Time	8.6
Reentry Time (Including casing/cementing)	3.2
Mechanical Repair Time (Contractor)	0.1
Stuck Pipe & Hole Trouble	3.6
ODP Equipment Problems	1.1
Other	0.7
Total Distance Traveled (nautical miles)	1919.0
Average Speed (knots)	8.5
Number of Sites	4
Number of Holes	10
Total Interval Cored (m)	2917.2
Total Core Recovery (m)	1655.2
Percent Core Recovered	56.7
Total Interval Drilled (m)	1884.3
Total Penetration (m)	4801.5
Maximum Penetration (m)	903.0
Maximum Water Depth (m from drilling datum)	3311.2
Minimum Water Depth (m from drilling datum)	2581.8

LEG 127 TOTAL TIME DISTRIBUTION



LEG 127 ON SITE TIME DISTRIBUTION



TECHNICAL REPORT

The ODP Technical and Logistics personnel aboard JOIDES Resolution for Leg 127 of the Ocean Drilling Program were:

Laboratory Officer:	Burney Hamlin
Assistant Laboratory Officer:	Matt Mefferd
Yeoperson:	Michiko Hitchcox
Curatorial Representative:	Peggy Myre
Computer System Managers:	Larry Bernstein Edwin Garrett
Electronics Technicians:	Michael Reitmeyer Barry Weber
Photographer:	Stacey Cervantes
Chemistry Technicians:	MaryAnn Cusimano Luis Pinto-Alvarez
X-ray Technician:	Donald Sims
Marine Technician/Underway Geophysics Lab:	Kenneth duVall
Marine Technician/Paleomagnetism Lab:	Nicholas Evans
Marine Technician/Underway Geophysics and Thin Section Labs:	Jenny Glasser
Marine Technician/Core Lab:	Jia-Yuh Liu
Marine Technician/Physical Properties Lab:	Mark Simpson
Marine Technician/Shipping/Storekeeper:	Charles Williamson

PORT CALL

JOIDES Resolution moored at Tokyo's Harumi passenger pier on 19 June. Crossover began immediately. A shipment of D-tubes arrived ahead of schedule and was loaded aboard in the rain. A representative from ARL began several days of troubleshooting and repairing the X-ray fluorescence unit.

Cores were offloaded on 20 June for refrigerated transport to the Gulf Coast Repository. A Hewlett Packard representative replaced a failed circuit board in the HP-1000 disk drive. The semi-annual radiation leak test on the GRAPE source was completed as required by the Radiation Safety Office at Texas A&M. A hard disk drive associated with the VAX cluster failed in port and a service call from DEC was requested, but Japanese Customs refused to allow the DEC representative aboard, and we sailed without a backup drive.

Texas A&M's Chancellor, Dr. William Mobley, visited the ship while he was in Japan to dedicate a new extension campus of Texas A&M. A shipboard luncheon was given for Dr. Mobley, ODP's A&M graduates, and the Japanese Aggie club.

The ODP storekeeper verified that all shipments for Leg 127 had been received by 23 June. This task was more difficult than usual, as ODP's and SEDCO's shipments had been unloaded elsewhere, mixed, and then delivered. Three navigation beacons that had been held by Japanese Customs since the Tokyo I portcall were delivered.

Prior to sailing on 23 June, long-delayed explosives for the pipe severing system were delivered to the ship. The area was formally cordoned off, with guards and fire watches prominently posted.

UNDER WAY

The last line was cast off as scheduled at 1600 hr, 23 June. *JOIDES Resolution* departed with the assistance of two harbor tugs and a pilot, beginning the 59-day cruise. Heavy traffic, fog, and rain accompanied the ship's departure from Tokyo harbor. Navigation tapes were initiated as soon as the ship cleared the harbor. Geophysical watches began at mid-morning on 24 June when the magnetometer was deployed. Fishing fleets and shallows on northerly passages along the coast and through the straits between Honshu and Hokkaido made it necessary to retrieve and deploy the magnetometer several times.

A sonobuoy survey was requested and initiated at Site 794, using LORAN C. Seismic gear was streamed with the magnetometer during the transits and surveys for Sites 795, 796 and 797 with good results. Transits (lines 2 and 3) were profiled at less than 8 kt to assure arrival on site when the GPS window was open. The transit to Site 797 (line 4) was made at 10 kt, resulting in slightly noisier seismic records.

The post-Site 796 survey was unusual in that while four GPS satellites were scheduled to be up at that time, position displays went soft for about 15 min. Radar ranges to the headlands on Hokkaido guided the ship into position for the survey line, and GPS then returned to normal.

LORAN C navigation was planned for the Site 797 survey but reception was poor. The bridge DECCA navigation aid was used to locate the site in a broad target area. DECCA is a shorter range version of the OMEGA type navigation system. A post-Site 797 survey was made, and a seismic line (5) was run over a Leg 128 proposed site during the transit to Pusan, South Korea.

GEOPLOT files were made of all transits and surveys to allow plotting of navigation, magnetics, and bathymetry as needed. LORAN C and DECCA positions were entered by hand from the bridge logs into the SMOOTH data base to get plots for two of the survey areas. Magnetometer and bathymetry plots were made using the GEOPLOT merging and plotting packages. Site positions were calculated using a 20/20 spreadsheet application.

OPERATIONS SUPPORT

Two of the sites occupied this leg required setting full-size reentry cones to achieve the scientific objectives of the leg. Reentry television and sonar equipment was maintained and deployed successfully in support of these objectives. A stuck bottom-hole assembly at the first site made it necessary to set up a new explosives shooting system, which allowed the pipe to be backed off above the BHA and left in salvageable condition.

The Water Sample Pressure and Temperature (WSPT) tool was deployed five times, acquiring five temperature measurements and three water samples. Heat flow measurements continued with 29 deployments of the Uyeda heat flow tool. Twenty-seven good measurements were collected. Multishot camera runs were completed every third core to orient piston cores.

The new experimental sonic core monitor (SCM) was deployed for the first time during XCB coring in Hole 797B. One run failed because of weak batteries but subsequent runs produced good data sets. The data were hand plotted for review and evaluation.

CORE LAB

The multisensor track (MST) worked well this leg and nearly all cores were processed. Many of the runs made were for magnetic susceptibility information. Software corrections to make 2-min density counts were initiated and were completed during the last day on site. An MST hardware and parts inventory was made and a block diagram of the device was drafted, to give users a quick overview of the instrument's configuration.

The numerous heat flow measurements made with downhole tools were supported by many laboratory thermal-conductivity measurements. "Therm Con" procedures were reviewed and refined by Dr. Marcus Langseth and software changes were relayed to ODP Science Operations for incorporation into new software being written. All physical properties instruments were used regularly and worked well.

Virtually every recovered section of core was processed using the cryogenic magnetometer. Parameters were selected to achieve the best compromise between resolution and measurement time. Processing was routine, except for a minor problem with

heavy cores in which the boat chain jumped the drive gear. An intermittent error in the y-axis console box was corrected by using the spare unit. A new file naming convention was introduced to PC and VAX software packages to making the files easier to work with. A "Users Guide to the Magnetism Lab Software" was written, and contributions were added to the "Emergency Procedures" document.

CHEMISTRY LAB

A plastic-lined sediment squeezer was introduced this leg. It is believed to be appropriate for trace metal analysis; continued comparison analyses using samples taken this leg will be done ashore. Samples for the plastic squeezer were prepared in a glove box using a nitrogen or helium atmosphere. Initial comparisons of analytical results from the plastic and standard stainless steel squeezers were made and show good agreement.

In general, all lab instruments were used heavily and performed well. The Rock Eval, Dionex and CNS commanded some extra maintenance and repair attention.

The acetylene gas safety alarm system, as presently adjusted, was found to be far too sensitive and non-selective for a lab with so many gases and solvents present. New calibration instructions were received near cruise end, and more gas standards were ordered to facilitate correcting the problem.

X-RAY LAB

The X-ray diffraction unit ran constantly, making full scans for the majority of determinations. The instrument was off only a few hours during the entire cruise, when a power controller board failed and was replaced. A potential time-saving feature using the X-ray fluorescence unit was explored to see if glass bead work could be replaced with powdered samples. Very encouraging results were achieved using powdered standards.

THIN SECTION LAB

A moderate number of thin sections was requested this leg, the majority from altered basalts or clay-bearing sediments. Special attention was given to slide preparation because of a problem with the lap wheels.

Ultraviolet epoxy was introduced to the lab on Leg 124. It has been useful in salvaging damaged slides and fixing materials considered delicate or in danger of being "plucked" in the grinding or polishing stages.

A fume exhaust fan was installed in the thin section lab, in addition to an activated carbon filter.

COMPUTER SERVICES

The VAX cluster was impaired slightly when a disk drive failed in port and could not be serviced (owing to a Japanese Customs restriction). The routine back-up scheme was adjusted to accommodate the failure, with no data loss.

Numerous requests were made by the shipboard party concerning Computer Services Group supported software. As changes were requested, the problems and proposed fixes were relayed to the beach for concurrence.

There were very few hardware problems with the PC clones or MACs this leg. The MACs continue to be the preferred computer for the majority of users, although some users ran into memory limitations.

A new systems manager was trained this leg.

ELECTRONICS SHOP

The ETs experienced another busy leg, giving support to the underway geophysics lab, downhole instruments, lab equipment, copiers, reentry TV and sonar, and general build- or fix-it requests. They were instrumental in the successful completion of the SCM trials.

Preparing the water sampler for rapid sequential deployment, and preparing for numerous deployments of the Uyeda heat flow probe made a significant demand on their time.

STOREKEEPER

A software problem was discovered that could result in assignment of confusing duplicate pallet numbers in a shipment. This was flagged for shore attention. Stock and reorder levels were changed to reflect heavier use of new chemistry lab instruments (AA, CNS).

It was noted that occasionally a shipped item is received that does not bring the item above the current reorder level, but it is not reflagged to be reordered, and could run out. Changes in Matman software are planned to keep this from happening.

SPECIAL PROJECTS

More replacement furniture for the fo'c'sle deck modification was received and stowed until the drydock period.

Wire safety windows were installed in the stairwell access doors in the lab stack, the entrances to the hold, and storage areas, thereby reducing a known safety hazard.

Open fibergrate was installed in a 3-ft wide strip under the core cutting racks on the core catwalk, to help keep the catwalk from becoming slippery.

SAFETY

A fire in the aft thyristor room resulted in the Captain mobilizing the Marine Emergency Technical Squad (METS) to carry fire gear and breathing-apparatus sets to the scene of the fire. Two of the METS team acquired front line experience keeping a high-voltage-transformer fire down, which allowed the engineers to work on restoring power to the ship. The thrusters and the drill floor were soon back to normal.

Regulated power was restored to lab equipment in 1-1/2 hr. Other than minor problems with information being lost temporarily in the oscilloscope supporting the Hamilton frame and with getting all the MST computers communicating with one another, no problems were noted.

The Captain and the Drilling Supervisor commended the METS for their professionalism. This team of technicians normally trains weekly with the SEDCO emergency squad.

LAB STATISTICS: LEG 127

GENERAL STATISTICS:

SITES	4
HOLES	10
INTERVAL CORED (M)	1655.2
CORE RECOVERED (M)	2917.2
NUMBER OF CORES	318
NUMBER OF SAMPLES	10414

SAMPLES ANALYZED:

INORGANIC CARBON (CaCO ₃)	609
TOTAL CARBON CNS	454
ROCK EVAL	353
WATER CHEMISTRY	152
THIN SECTIONS	125
XRF (MINOR & MAJOR)	60
XRD	455
DISCRETE PALEOMAG SAMPLES	156
WHOLE CORE PASS THROUGH CRYOMAG	1165
GRAPE2	240
PHYS PROPS VELOCITY	346
INDEX PROPERTIES	1071
THERMAL CONDUCTIVITY	1050

UNDERWAY GEOPHYSICS (THROUGH LINE 4)

TOTAL NAUTICAL MILES TRANSIT	1249
BATHYMETRY, MAGNETICS	1036
SEISMICS	713

DOWNHOLE TOOLS:

HEAT FLOW RUNS (UYEDA)	29
HEAT FLOW AND WATER SAMPLER RUNS	5

OCEAN DRILLING PROGRAM
 SITE SUMMARY REPORT
 LEG 127

HOLE	LATITUDE	LONGITUDE	DEPTH METERS	NUMBER OF CORES	METERS CORED	METERS RECOVERED	PERCENT RECOVERED	METERS DRILLED	TOTAL PENETRATION	TIME ON HOLE	TIME ON SITE
794A	40-11.41N	138-13.86E	2821.7	37	351.3	302.2	86.0	.0	351.3	69.00	
794B	40-11.40N	138-13.87E	2821.7	27	249.2	87.4	35.0	299.8	549.0	104.25	
794C	40-11.40N	138-13.86E	2820.0	14	93.9	33.2	35.3	559.8	653.7	182.50	355.75
795A	43-59.23N	138-58.03E	3311.2	39	364.9	258.3	70.7	1.0	365.9	757.50	
795B	43-59.24N	138-57.89E	3310.0	41	397.0	188.9	47.5	365.2	762.2	146.75	222.50
796A	42-50.93N	139-24.67E	2581.8	27	242.9	155.3	63.9	.0	242.9	49.75	
796B	42-50.92N	139-24.85E	2633.8	33	293.8	85.3	29.0	171.1	464.9	117.50	167.25
797A	38-36.94N	134-32.16E	2873.6	1	9.5	9.7	102.1	3.4	12.9	8.00	
797B	38-36.94N	134-32.16E	2873.6	53	495.7	370.7	74.7	.0	495.7	94.00	
797C	38-36.93N	134-32.18E	2876.0	46	419.0	164.2	39.1	484.0	903.0	336.00	438.00
TOTALS:				318	2917.2	1655.2	56.7	1884.3	4801.5		1183.50

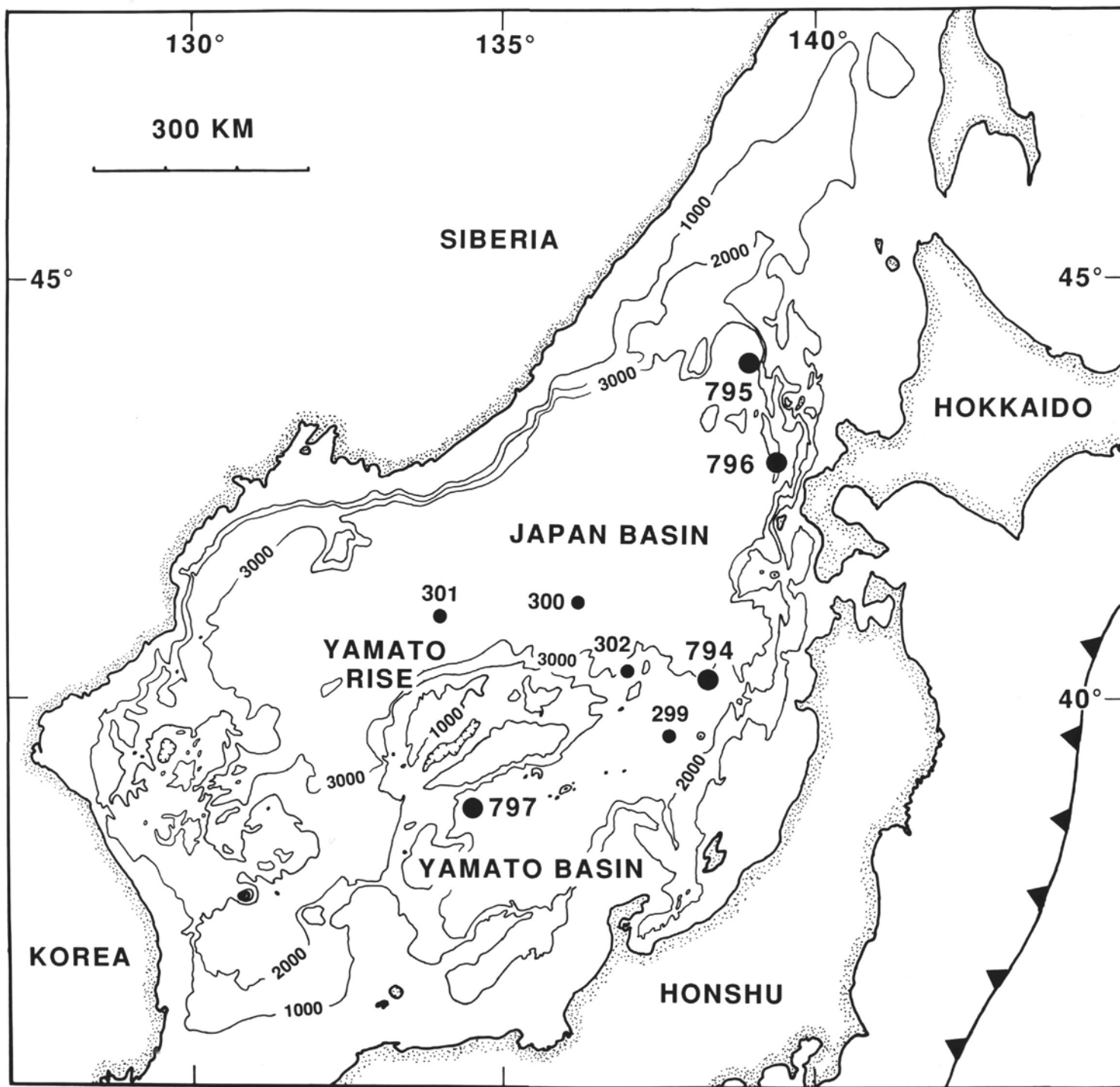


Figure 1. Bathymetric map of the Japan Sea; bathymetric contours are in meters. ODP Leg 127 sites are shown as large dots; DSDP Leg 31 sites are shown as smaller dots. Toothed line represents the Japan Trench.

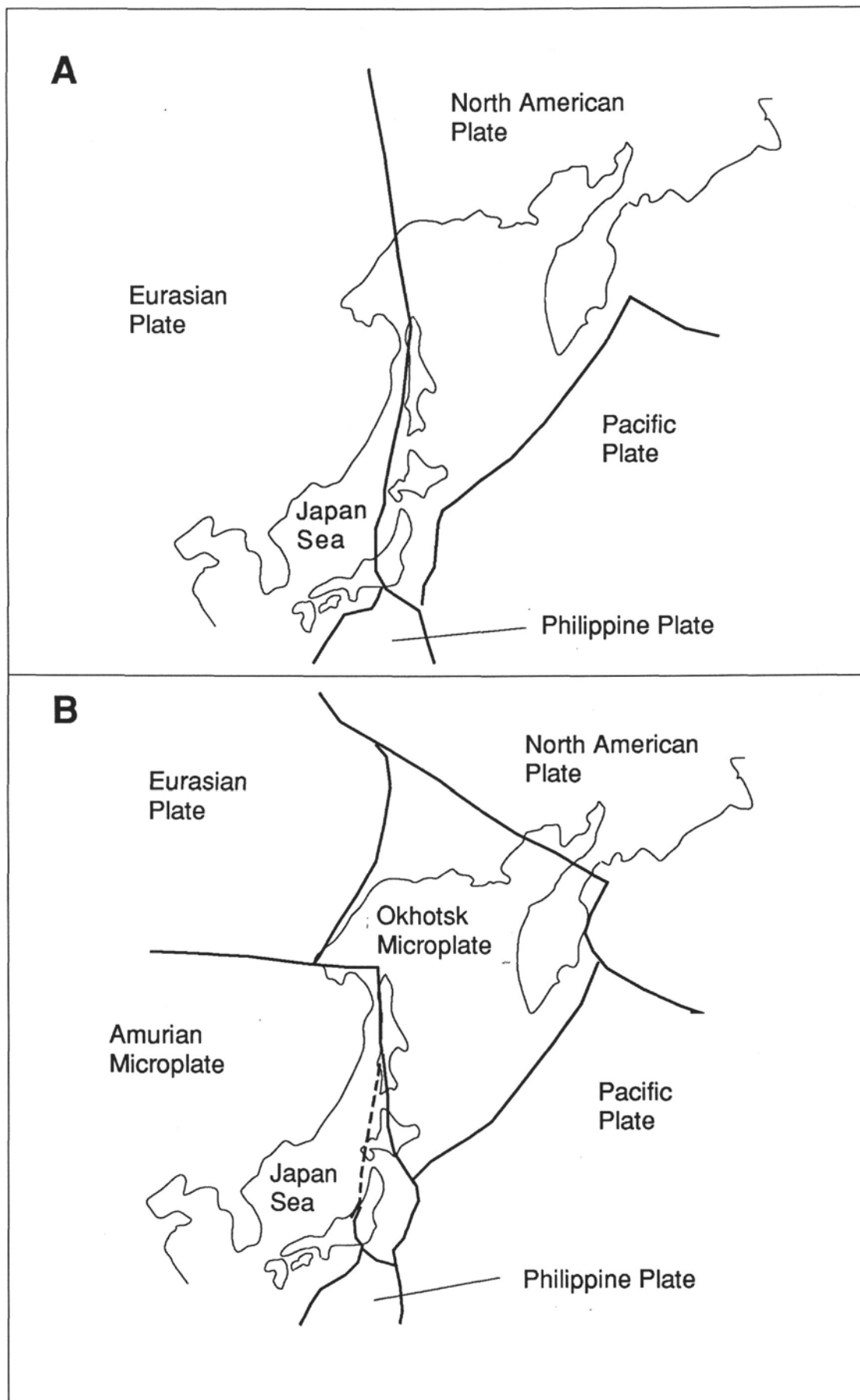


Figure 2. Map showing major lithospheric plates (A) and microplates (B) in the Japan Sea region. See text for references.

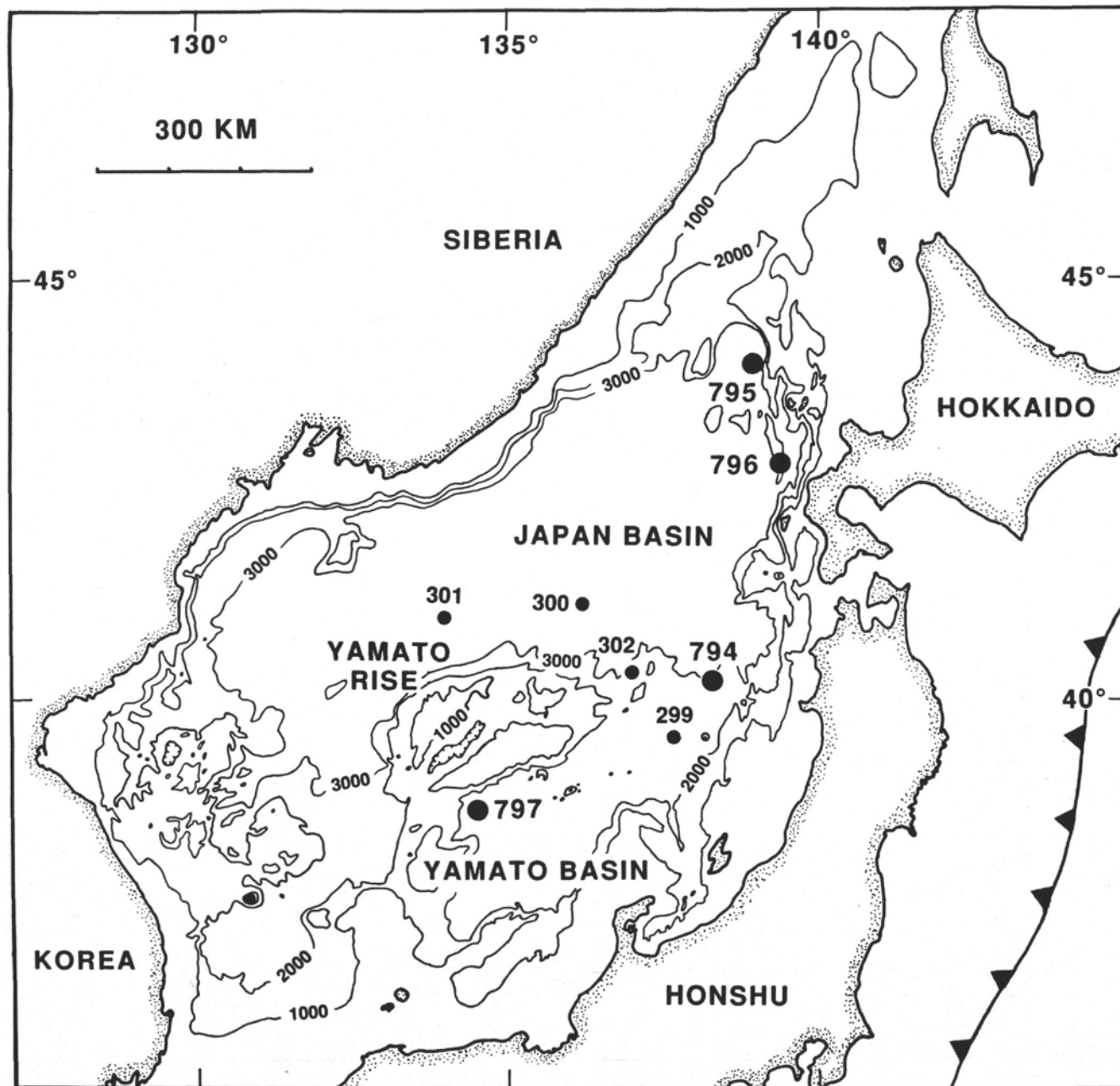


Figure 1. Bathymetric map of the Japan Sea; bathymetric contours are in meters. ODP Leg 127 sites are shown as large dots; DSDP Leg 31 sites are shown as smaller dots. Toothed line represents the Japan Trench.

OCEAN DRILLING PROGRAM
 SITE SUMMARY REPORT
 LEG 127

HOLE	LATITUDE	LONGITUDE	DEPTH METERS	NUMBER OF CORES	METERS CORED	METERS RECOVERED	PERCENT RECOVERED	METERS DRILLED	TOTAL PENETRATION	TIME ON HOLE	TIME ON SITE
794A	40-11.41N	138-13.86E	2821.7	37	351.3	302.2	86.0	.0	351.3	69.00	
794B	40-11.40N	138-13.87E	2821.7	27	249.2	87.4	35.0	299.8	549.0	104.25	
794C	40-11.40N	138-13.86E	2820.0	14	93.9	33.2	35.3	559.8	653.7	182.50	355.75
795A	43-59.23N	138-58.03E	3311.2	39	364.9	258.3	70.7	1.0	365.9	757.50	
795B	43-59.24N	138-57.89E	3310.0	41	397.0	188.9	47.5	365.2	762.2	146.75	222.50
796A	42-50.93N	139-24.67E	2581.8	27	242.9	155.3	63.9	.0	242.9	49.75	
796B	42-50.92N	139-24.85E	2633.8	33	293.8	85.3	29.0	171.1	464.9	117.50	167.25
797A	38-36.94N	134-32.16E	2873.6	1	9.5	9.7	102.1	3.4	12.9	8.00	
797B	38-36.94N	134-32.16E	2873.6	53	495.7	370.7	74.7	.0	495.7	94.00	
797C	38-36.93N	134-32.18E	2876.0	46	419.0	164.2	39.1	484.0	903.0	336.00	438.00
TOTALS:				318	2917.2	1655.2	56.7	1884.3	4801.5		1183.50